PRISE - FORCE MODELS FOR DRAINED AND UNDRAINED STEADY STATE ICE SCOURING

Prepared for

PRISE Participants

Prepared by

C-CORE

C-CORE Publication 98-C33
December 3, 1998

C-CORE
Memorial University of Newfoundland
St. John's, NF. A1B 3X5, Canada
Tel. (709) 737-8354 Fax. (709) 737-4706

The correct citation for this report is:

Walter, D. J. and Phillips, R. (November 1998). "PRISE - Force models for drained and undrained steady state ice scouring". Contract report, C-CORE Publication 98-C33.

QUALITY CONTROL REPORT

Client:	PRISE Participants
Project:	Risk of ice damage to seabed facilities
Client's Contract Ref:	
C-CORE Cost Centre:	340469

Document Title:	Force models for drained and undrained steady state ice scouring
C-CORE Pub. No.:	98-C33
Prepared By:	D. J. Walter and R. Phillips
Date:	November, 1998

Reviewers	Document Accepted Date — Signature
Technical Accuracy	Nov. 22/98 Shawn Hurley Dec 2nd / '98 Tony Kim
Syntax	
Layout & Presentation	
General Evaluation	3/12/98 R. P...

Approval for Release

Date: Dec 3/98.

President & CEO

TABLE OF CONTENTS

LIST OF TABLES

LIST OF FIGURES

1.0 INTRODUCTION

This report was written to document the development of two numerical models for predicting soil forces during steady state ice scouring conditions. A brief review of existing scour models is first carried out which provides a description of various existing models including a summary of the assumptions used in formulating the models.

A detailed description is provided of the formulation of two C-CORE models: The first model is suitable for analysing scour forces in fully drained soils using effective strength parameters, c' and ϕ'. The second model is suitable for analysing scour forces in undrained conditions with ϕ=0 and using the undrained strength, c_u.

Comparisons are made between the C-CORE models and other existing models, as well as with the results of scour experiments carried out on a centrifuge for the Pressure Ridge Ice Scour Experiment (PRISE).

Finally, parametric analyses are carried out to determine how the computed scour forces vary with changes to key parameters.

2.0 REVIEW OF ICE SCOUR MODELS

2.1 Chari Model

2.1.1 Model description

The Chari model for ice scouring is an energy model that balances the energy available to drive an iceberg against the resistance to scouring provided by a sloping seabed. Energy is computed considering the mass of the berg and environmental factors such as current, current drag, and wind. Resistance to scouring is determined based on a passive pressure mechanism at the face of the scouring berg, and is dependent on the length, depth and width of the scour, the surcharge developed due to the scouring berg, the effective unit weight of the soil, and the shear strength of the soil (see Figure 1). The original model was presented by Chari (1975) and extensions, refinements, and validations of the model have since been extensively published (Chari and Guha 1978, Chari and Muthukrishnaiah 1978, Chari 1979, Chari 1980, Chari et al 1980, Chari and Peters 1981, Chari and Green 1981, Green 1984).

2.1.2 Formulation of model

The problem geometry and the location and orientation of scour forces are shown in Figure 2. A summary of symbols and abbreviations used in the Chari model is provided in Table 1. The following paragraphs provide a summary of the assumptions used in formulation of the Chari scour model.

- The iceberg is a prismatic block, rectangular in plan with its short side perpendicular to the travel direction.

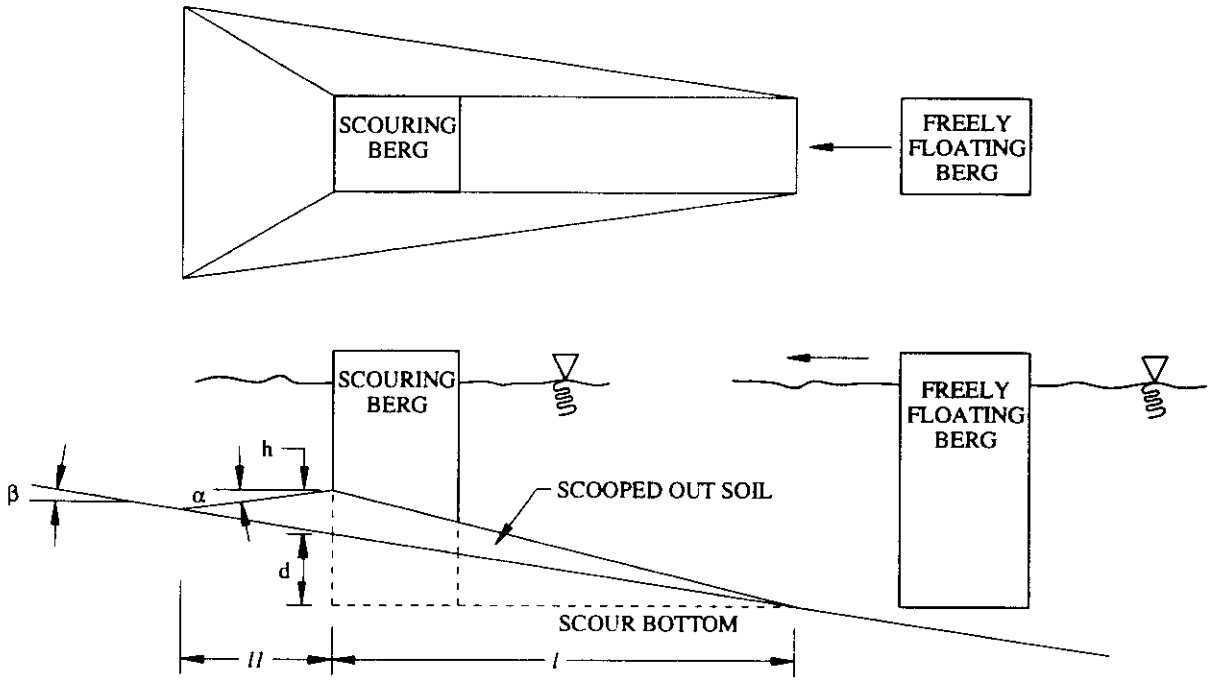

Figure 1. Chari Model - Idealized scouring mechanism

- The strength of the ice is greater than the strength of the soil.
- The bottom sediments are assumed soft and yielding.
- The berg moves with a constant draft (i.e. horizontally into the slope).
- Grounding occurs only when the berg meets a bank or a slope.
- Berg movement is assumed to be normal to the slope during grounding.
- There is no volume change associated with the soil going from its original to the displaced condition.

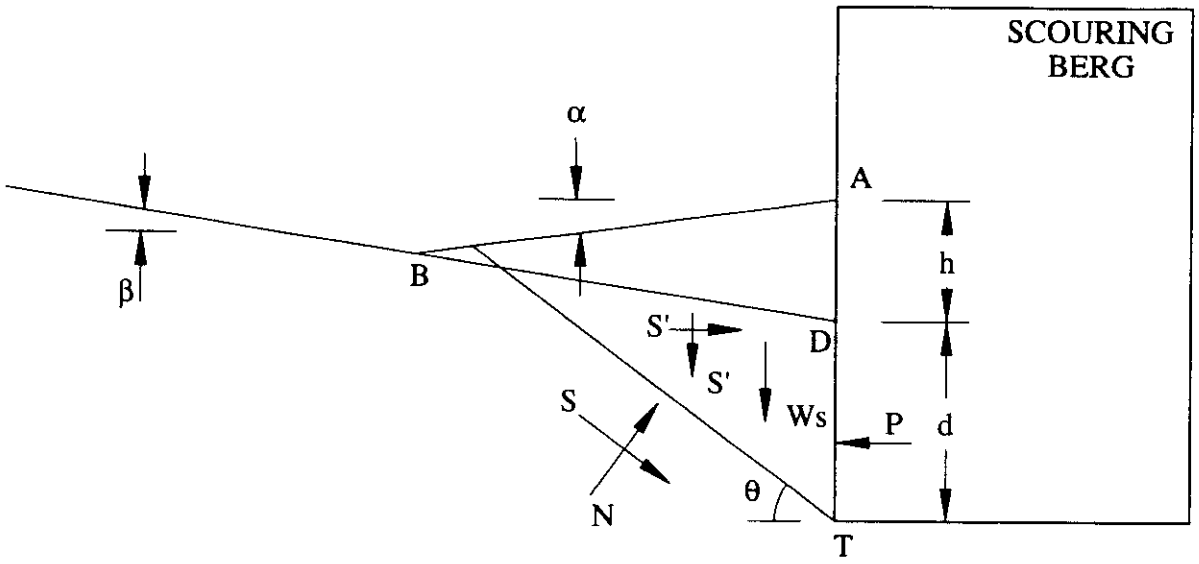

Figure 2. Chari Model - Scour forces and geometry

- It is assumed that the soil is cohesive. The friction angle is considered to be small and is neglected.

- The base shear is assumed to be small in comparison with the passive resistance at the front of the berg and is neglected (i.e. constant draft with no downward pressure).

- The weight of the passive wedge of soil includes a surcharge due to the displaced soil.

- The slope of the sea floor, tan β, and the slope of the frontal mound, tan α, are assumed to be very small in calculating the total soil resistance (i.e. horizontal slopes).

- The height of the frontal mound, h, is assumed to vary linearly with scour depth, d (i.e. h = constant · d).

- The wedge angle, θ, is assumed to be equal to 45° for cohesive soil (i.e. 45 - ϕ/2, where $\phi = 0°$).

- It is assumed that the work carried out in accelerating the soil wedge to the velocity of the berg is negligible compared to the initial kinetic energy of the iceberg and is neglected.

2.1.3 Governing equations

At any instant during scouring, the frontal resistance to the iceberg is calculated as:

$$P = \frac{\gamma'(h+d)^2}{2}B + \frac{2\tau dB}{\sin 2\theta} + \frac{\tau d^2}{\sqrt{2}}(1+\cot\theta)$$

The equation for iceberg scour is given as:

$$F_{wd}L + \frac{1}{28}F_{cd}L + \frac{1}{2}MV^2 = \frac{1}{6}\gamma'(H+D)^2BL + \tau DLB + \frac{\sqrt{2}}{3}\tau D^2L + 0.1\gamma'BD^2L$$

Table 1. Summary of symbols and abbreviations used in Chari model

Parameter	Description
F_{wd} =	wind drag force = $\frac{1}{2}\rho_A A(C_{Dfa}A_F + C_{Dra}A_{RS})V_w^2$
F_{cd} =	current drag force = $\frac{1}{2}l_w(C_{Dfw}A_F + C_{drw}A_{RK})\lvert V_I - V_C\rvert(V_I - V_C)$
L =	final length of scour
M =	mass of berg
V =	initial velocity of berg at the commencement of scouring
C_D =	drag coefficient
ρ =	density
A =	cross-sectional area on which the drag force acts
γ' =	submerged unit weight of ocean bed sediment
H =	final height of scoured soil at the front face of berg
D =	final depth of scour
B =	width of berg perpendicular to the direction of scour
τ =	shear strength of ocean bed sediment
h =	height of scoured soil at the front face of the berg at any instant of scouring
d =	depth of scour at any instant of scouring
α =	angle of the inclined face of ploughed soil in front of berg
β =	bottom slope angle
θ =	shearing angle on passive wedge at leading edge of berg
ℓ =	scour length
Λ =	distance to end of spoil pile in front of scour
S =	shear resistance along base of wedge
N =	normal force at base of wedge
Ws =	weight of soil wedge
S' =	side shear resistance
P =	total soil resistance

2.2 Kioka Model

2.2.1 Model description

The Kioka sand model was developed for the case where sea ice scrapes the sandy sea floor while it is pushed by the offshore ice field to a shallow sea area. A description of experiments carried out to simulate this process was provided by Kioka and Saeki (1995) and Kioka et al (1998). A view of the experimental setup used in the model experiments is provided in Figure 3. The model incorporates passive resistance on the front and sides of the scour, and sliding resistance on the base of the ice. The scour forces are determined by solving the equations of motion in the horizontal and vertical direction and the stability conditions of the ice.

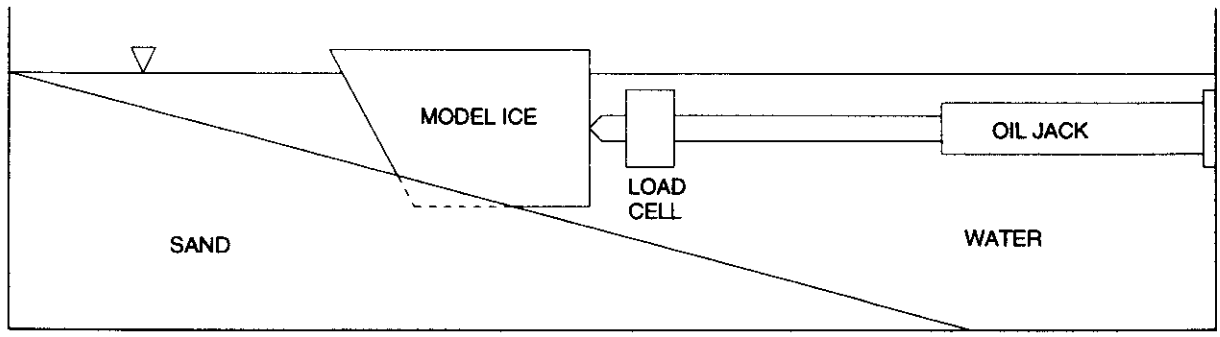

Figure 3. Kioka Scour Model - Experimental setup for model experiments

2.2.2 Formulation of model

A summary of the symbols and abbreviations used in describing the Kioka ice scour model is provided in Table 2. The scour geometry and associated forces are shown in Figure 4. The Kioka ice scour model was formulated using the following assumptions:

- The scouring model developed is for sands.

- The sea floor bottom is sloped.

- The scouring berg is rectangular parallelopiped in shape with a vertical or sloping scouring face.

- The scouring berg is assumed to be moving at a constant velocity.

- Neglect consecutive changes in the internal friction angle, nonuniformity of relative density of sand, and the problems with permeability.

- Forces considered include earth pressure acting on the front and sides of the model, the subgrade reaction and dynamic friction acting on the bottom of the model ice, and the buoyancy of the model.

- It is assumed that all of the sand moved by the model is deposited on the front part of the model ice.

- Passive pressure on the front of the model is determined using the Coulomb passive pressure formulation.

- Passive pressure on the sides of the model is determined using the Rankine passive pressure formulation.

- The ice moves vertically and horizontally during scouring. It is assumed that the model ice moves along a function $Y=\zeta(x)$ called the gouging curve.

- When the gouging curve is known, the ice force is obtained from the equations of motion in the horizontal and vertical directions and the stability conditions of the ice.

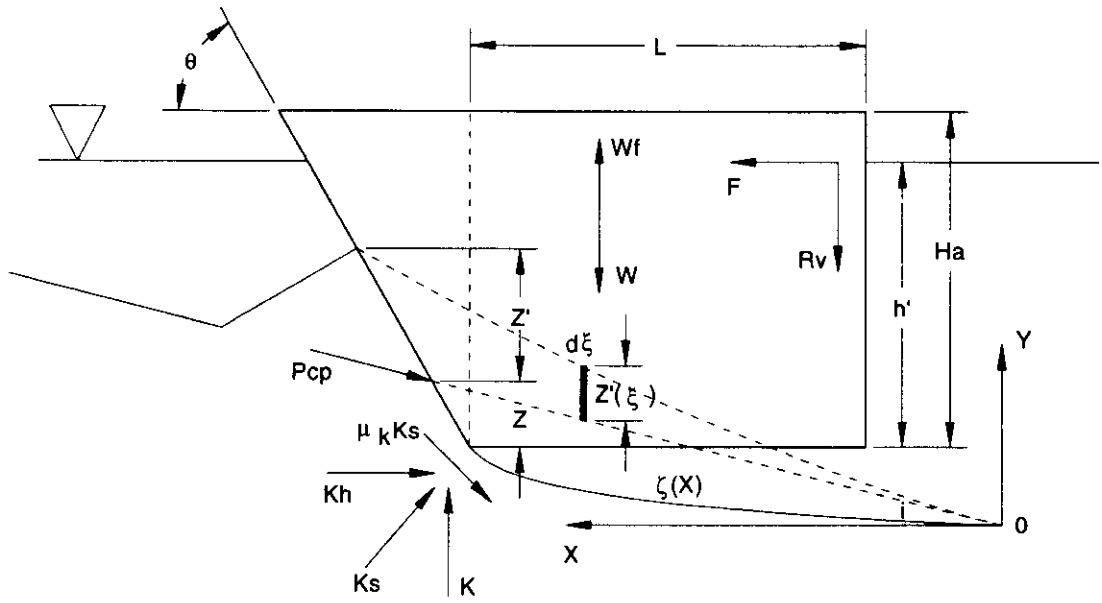

Figure 4. Kioka Model - Scour forces and geometry used in model

2.2.3 Governing equations

1) Earth pressure on front of model (P_{cp})

$$P_{cp} = \tfrac{1}{2}\,\gamma\, H^2\, B\, K_{cp}$$

2) Earth pressure on sides of model (P_s)

$$P_s = \gamma\, K_{ps} \left[\int_K^X \int_0^{Z'(\xi)} \eta \, d\eta \, d\xi \;+\; \int_X^{X+(Z+Z')\tan\theta} \int_{\xi\cot\theta}^{Z'(\xi)} \eta \, d\eta \, d\xi \right]$$

where $K_{ps}=\tan^2(45+\phi/2)$

3) Accumulation of sand during the movement of the ice, Z'(x)

$$Z'(X) = \frac{1}{N}\left\langle \exp(-\frac{\cot\beta}{N}X)[\int \exp(\frac{\cot\beta}{N}X)\{X\tan i - \zeta(X)\} + C]dX \right\rangle^{1/2}$$

4) Equation of motion in the horizontal direction

$$F - P_{cp}\cos(\alpha-\delta) - \mu_k(2P_s + K) - K\frac{d\zeta}{dX} = 0$$

5) Equation of motion in the vertical direction

$$-MV_o^2\frac{d^2\zeta}{dX^2} + K(1 \pm \mu_k\frac{d\zeta}{dX}) - W + (h'B + \frac{1}{2}h'^2\tan\theta)B\gamma_w \pm F_v - P_{cp}\sin(\alpha-\delta) = 0$$

6) Vertical frictional force acting on back of ice at point of connection with ram

$$F_v = \frac{1}{L}\left[(h'B + \frac{1}{2}h'^2\tan\theta)B\gamma_w L_G - WL_G - \frac{H}{3}P_{cp}\cos(\alpha-\delta) - MV_o^2\frac{d^2\zeta}{dX^2}L_G - M_B + (h-\zeta(X))F\right]$$

The unknown quantities from the above formulae are F, K and F_v and the above equations are solved for these unknowns.

Table 2. Summary of symbols and abbreviations used in Kioka scour model

Parameter		Description
P_{cp}	=	passive earth pressure on front of model
K_{cp}	=	Coulombs passive pressure coefficient
P_s	=	passive earth pressure on sides of model
K_{ps}	=	Rankine passive pressure coefficient
γ'	=	submerged unit weight
H	=	$Z\,[(\cos(i+\theta)\cos i) / (\cos(i+\alpha)\cos\theta)]$
B	=	width of the ice
i	=	slope of seafloor from horizontal
ϕ	=	friction angle of soil
θ	=	angle of inclination of the front side of the ice
δ	=	friction angle between ice and soil
β	=	angle between face of ice and seafloor
Z'	=	$f(\xi)$ = accumulation height of sand
Z	=	gouging depth
$\zeta(X)$	=	gouging curve
W	=	weight of the model ice
W_f	=	buoyancy
K	=	subgrade reaction in the vertical direction
F	=	ice force
F_v	=	frictional force in the vertical direction between the model ice and the connector
h'	=	draft of the model ice
H_a	=	height of the model ice
μ_k	=	coefficient of dynamic friction between the model ice and the sand

2.3 Been Model

2.3.1 Model description

The Been ice scour model calculates the energy of the advancing ice feature and energy dissipated by the work carried out due to scouring of the sea floor over small prescribed displacement intervals. After each increment of ice movement, a force equilibrium calculation is performed to determine the magnitude of ice uplift. Soil resistance is determined based on a passive pressure rupture zone created at the front of the scouring ice. The model uses effective strength parameters and assumes drained conditions during scouring. The model was developed by Golder Associates Ltd. and is described by Been et al (1990a and 1990b).

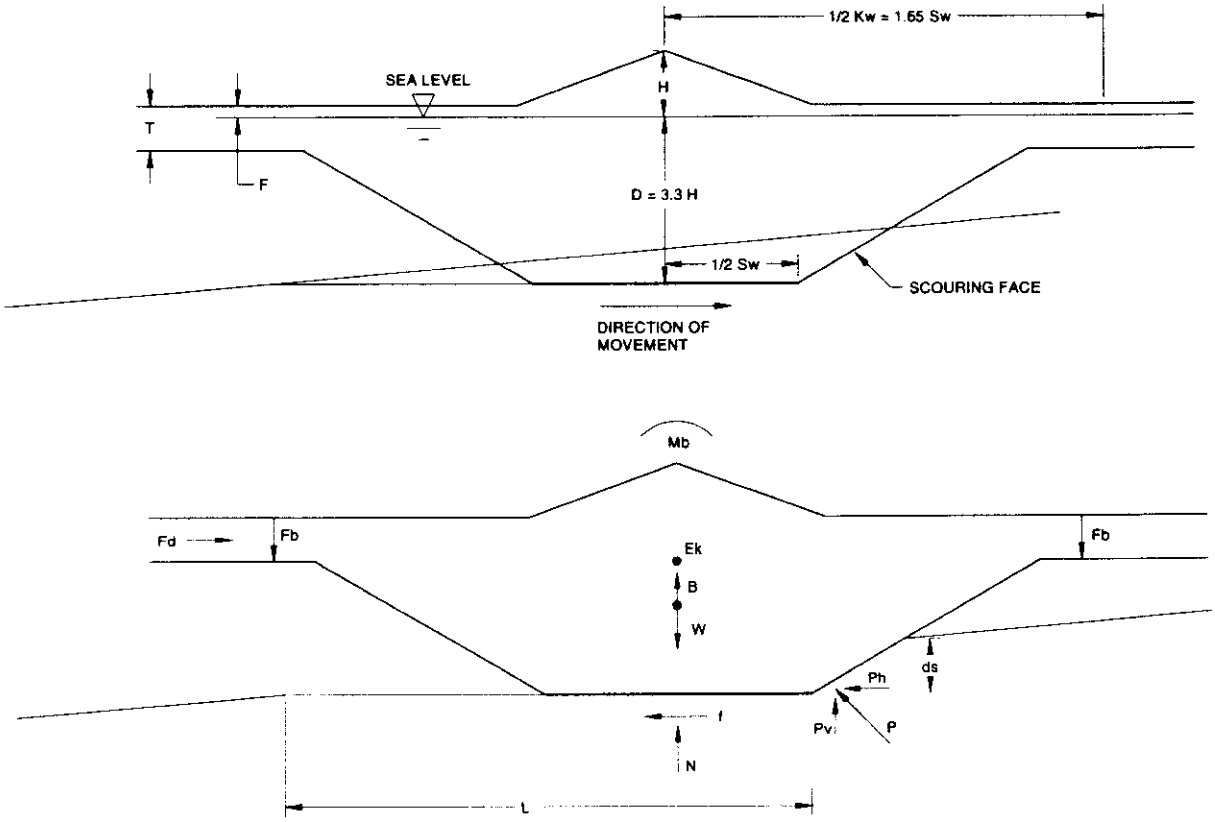

Figure 5. Geometry and forces used in Been model (Been et al 1990b)

2.3.2 Formulation of model

The scour model is based on the free body diagram for an idealized ice feature moving into a sloping seabed as shown in Figure 5. The symbols and abbreviations used in formulating the Been model are summarized in Table 3. The assumptions used in formulating the scour model are briefly summarized in the following paragraphs.

- Scouring occurs until the initial kinetic energy and work done by the driving forces is expended through work done on the seabed, or until the soil resistance exceeds the strength of the ice keel.

- The sea floor is sloping and the scour occurs perpendicular to the slope.

- The movement of keels are mostly horizontal and largely controlled by the parent floe.

- The ploughing face may have a very low angle to the horizontal (generally <30°).

- Ice keel widths are generally large when compared to keel depth. Due to the large keel width:depth ratio the three-dimensional affects are considered to be small and are neglected in the model.

- A quasi-dead wedge of soil forms in front of the ice keel and is carried with the ice during scouring. The net effect is to increase the cutting angle of the scouring ice keel.

- As the ice keel translates, soil is pushed up and out in front of the scour eventually forming a stable mound configuration. Additional soil feeding in from the failure

zone is cleared from the path of the ice to berms on either side of the scour.

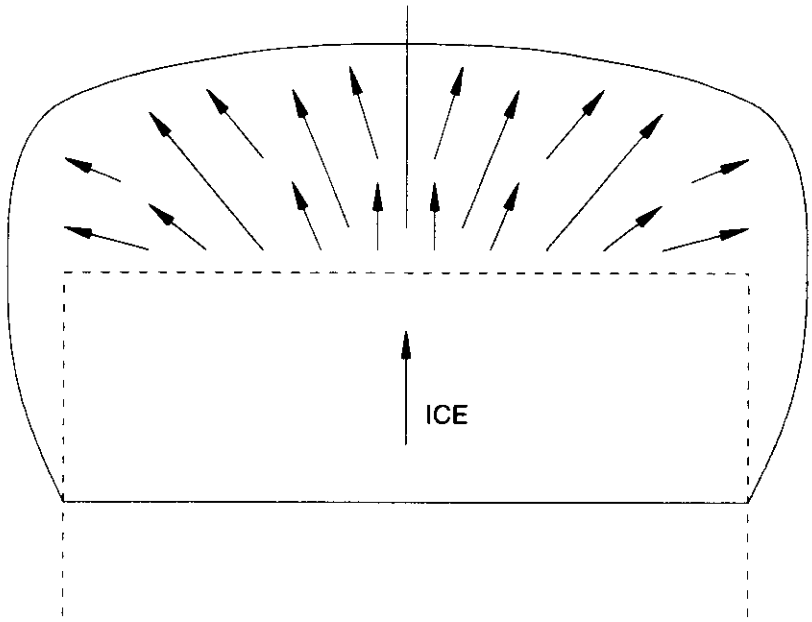

Figure 6. Plan view of ice scour mechanism assumed for Been model

- The edge effects and ploughing motion combine to form a spoon shaped failure zone (See Figure 6).

- As the ice continues to scour, the vertical force applied by the soil on the ice will increase, causing upwards movement of the ice keel so that vertical force equilibrium of the ice mass is maintained.

- The passive resistance at the front of the scouring berg is determined using a method modified from that proposed by Sokolovski (1965). The Sokolovski stress field method is a lower-bound plasticity solution assuming two-dimensional plane strain conditions. The Mohr-Coulomb failure criterion is satisfied throughout the soil mass and each point within the mass is in a plastic state. The stresses within the ruptured

zone are taken to be in equilibrium with the boundary stresses applied to the soil. The stress distribution is found by satisfying the equations of equilibrium within the failure zone.

- The Sokolovski approach is modified to include the formation of dead wedges of soil within the failure zone which are calculated in a similar manner to that described by Hettiaratchi and Reece (1975).

- Not all of the features of the model are fully developed in the software provided by Golder Associates (Been et al 1990b). It appears that the program is configured to calculate the vertical and horizontal forces due to the passive pressure failure at the front of the berg (including an adjustment to the scour depth to account for the vertical component of the passive resistance). The program does not appear to calculate the normal soil reaction force below the keel or the sliding resistance on the base of the scour due to the normal force.

2.3.3 Governing equations

The governing equations for the Been model are not explicitly documented in the literature. The source code has been published (Been et al 1990b) for a computer program written to carry out scour analysis using the model. If required, the governing equations could be backed out of the source code. A flow chart for the computer program is shown in Figure 7.

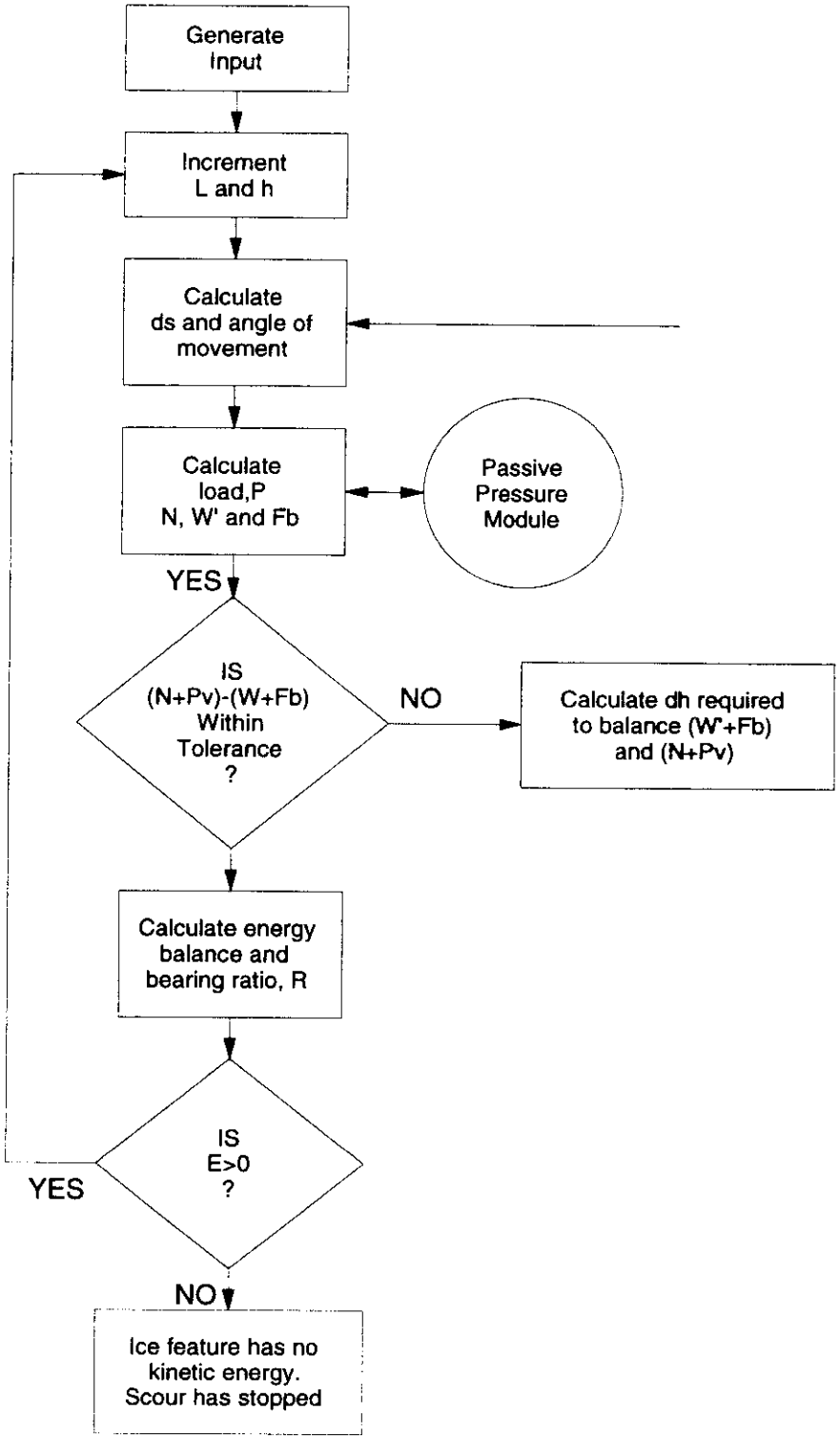

Figure 7. Calculation steps for Been model (Been et al 1990b)

Table 3. Summary of symbols and abbreviations used in Been scour model

Parameter		Description
H	=	sail height (typically 1 to 8 metres)
D	=	keel depth
Sw	=	sail width
Kw	=	keel width
T	=	ice thickness
F	=	freeboard
ds	=	depth of scour
L	=	length of scour
Ek	=	kinetic energy of berg
Fd	=	drag force on ice due to wind and current
P	=	passive resistance of soil
N	=	normal force on ice from soil outside the "passive zone"
f	=	friction between ice and soil
Fb	=	flexural force supplied by surrounding ice
h	=	height of berg above free floating level
Mb	=	righting moment due to bouyancy
W	=	weight of ice feature
B	=	bouyancy force
S	=	slope gradient

2.4 Surkov Model

2.4.1 Model description

Surkov's (1995) ice scour model is very similar in some ways to the Chari model. Both models involve the horizontal translation of an ice feature into a sloped seabed. Figure 8 shows the mechanisms assumed for the Surkov model. The primary differences between the Surkov model and the Chari model is that (1) the Surkov model is for frictional soil rather than cohesive soil, and (2) the Surkov model assumes that all of the displaced soil remains in front of the scouring berg.

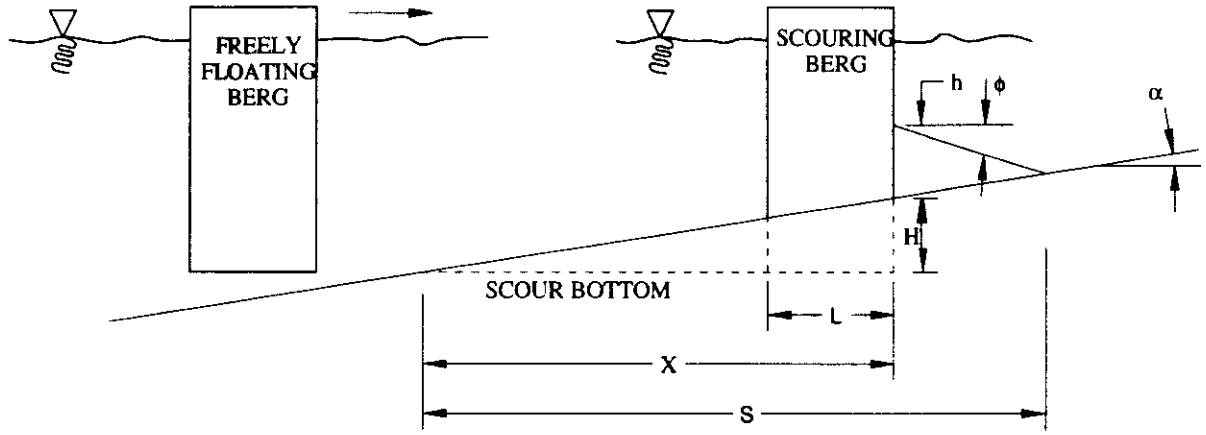

Figure 8. Idealized scouring mechanism assumed for Surkov model

2.4.2 Formulation of model

The problem geometry and the location and orientation of scour forces are shown in Figure 8. A summary of symbols and abbreviations used in the Surkov model is provided in Table 4. The following paragraphs provide a summary of the assumptions used in formulation of the Surkov scour model.

- The ice scour model calculates soil resistance based on the passive pressure calculated for a wedge of soil at the leading edge of the scouring berg subjected to a surcharge due to the creation of a frontal mound.

- It is assumed that the seafloor slope is constant.

- Scour occurs in a horizontal direction into the slope. There is no vertical movement associated with the scour.

- Assume that the cohesion of the soil is small and can be neglected. Only the friction angle is used in determining the passive pressure coefficient.

- The width of scour (B) is assumed to be much greater than the depth of scour (H), therefore, all of the soil displaced during scour is assumed to contribute to the height of the frontal mound (i.e. no lateral displacement of soil).

- The friction angle of soil in the berm is equal to the angle of repose of the soil.

- An equivalent height of surcharge is assumed that is 0.15 times the height of the mound (see Figure 9).

- Side shear is assumed to be a small component of the overall soil resistance and is neglected.

- Neglect friction along bottom of ice keel.

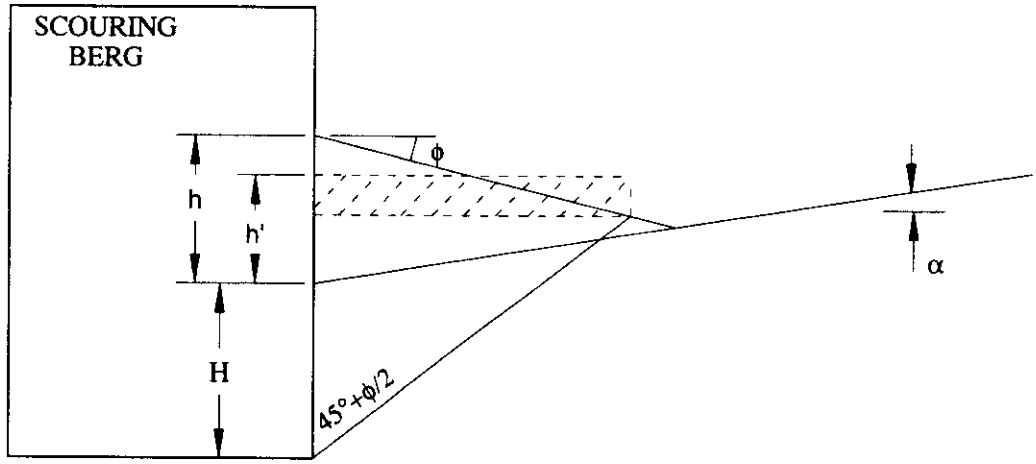

Figure 9. Equivalent surcharge used in passive pressure calculation for Surkov model

2.4.3 Governing equation

The horizontal scouring force for some scour length, x, is calculated using the following equation:

$$Fc(x) = \left[\frac{1}{2}\gamma\left(\tan\alpha + 0.85\sqrt{\tan\alpha\tan\phi + \tan^2\alpha}\right)^2 K_p B\right]x^2$$

Table 4. Summary of symbols and abbreviations used in Surkov model

Parameter		Description
Fc(x)	=	scour force for a specified scour length, x
B	=	width of scour
α	=	slope of seafloor
ϕ	=	friction angle of soil
Kp	=	passive pressure coefficient, (Rankine)
X	=	horizontal scour distance
H	=	scour depth = x tan α
L	=	length of berg
h	=	height of frontal mound (approximated as uniform surcharge)
h'	=	equivalent height of surcharge
γ	=	unit weight of soil

2.5 Other Scour Models

There have been scour models developed and physical model tests carried out in addition to those described in the previous sections of this review. Some of these include the work-energy FENCO (1975) model, which is quite similar to the Chari model; the Beloshapkov-Marchenko model (Beloshapkov et al, Beloshapkov and Marchenko 1998) which is extremely complex mathematically; and others (Dunwoody et al 1984, Bea et al 1985, etc). A scour model, based on the Chari model, has been used by Truskov and Surkov (1991) to predict scour depths in the northern Sakhalin offshore.

3.0 C-CORE MODEL FOR FULLY DRAINED SCOURING

3.1 Model Description

The C-CORE ice scour model for c' - ϕ' soil under drained conditions, is based on the assumption of steady state scour conditions where the scour force, the scour depth, the scour width, and the size of the frontal mound and side berms remain constant over large scour distances (often in the order of 1000's of metres in length). Scour resistance is generated by the soil through several mechanisms including, (1) passive resistance at the front of the scouring berg, (2) shear resistance at the base of a dead wedge created in front of the scouring berg, and (3) shear resistance on the two sides of the dead wedge. These mechanisms are shown schematically in Figure 10.

3.2 Formulation of Ice Scour Model

The assumed scour geometry and the location of the forces are shown on Figure 11. The magnitude, location, and orientation of the resultant soil reaction forces, R_h and R_v, can be determined using the scour model developed on the following pages. A summary of symbols and abbreviations used in formulating the scour model is presented in Table 5 located at the end of section 3.

The methodology and assumptions used in formulating the scour model are summarized as follows:

- The base of the scour is parallel with the sea floor (this is equivalent to assuming that the sea floor is horizontal and the scour depth is constant).

- Steady state scouring conditions are assumed where:
  - scour depth, D, is constant,
  - scour width, B, is constant,

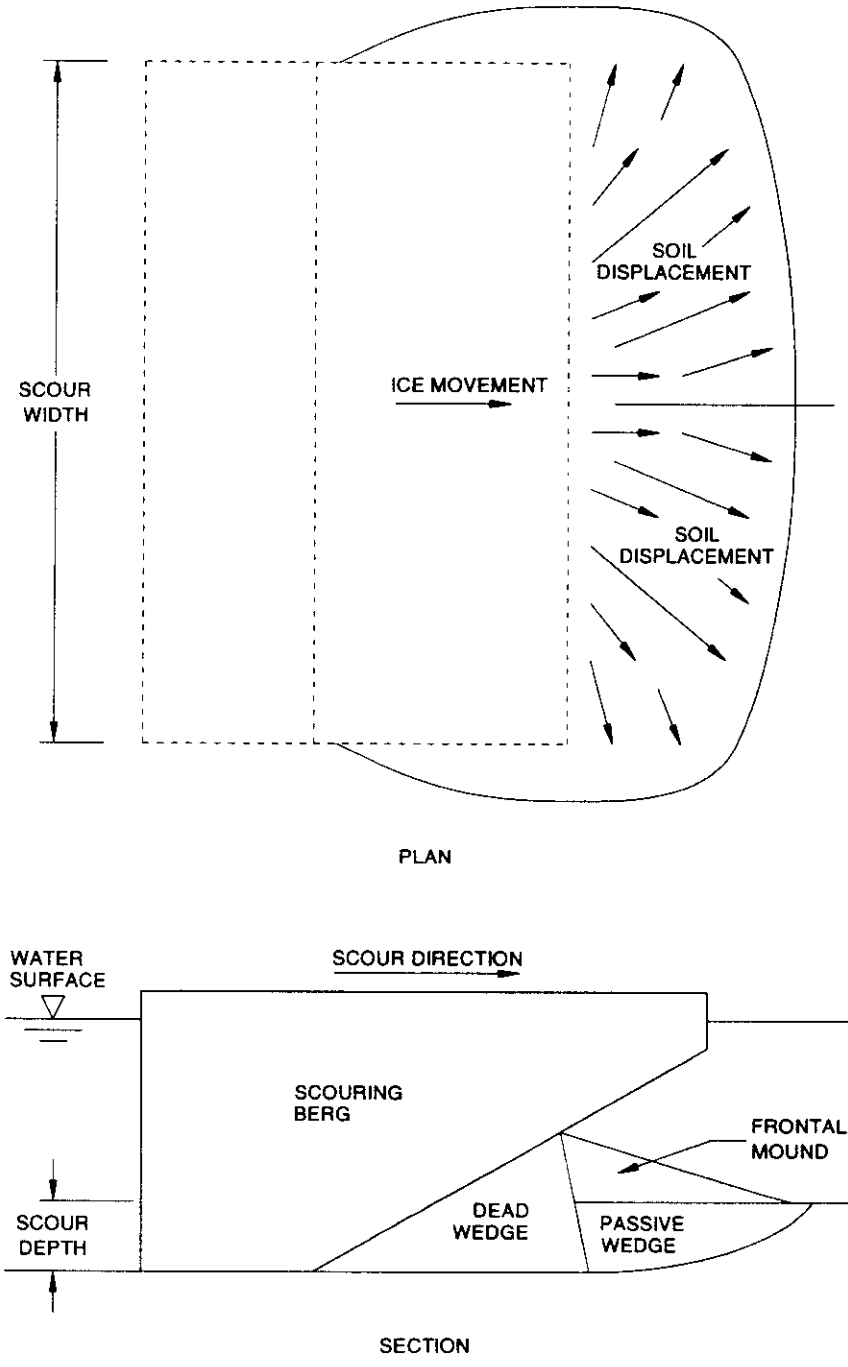

Figure 10. Mechanism for C-CORE c' - ϕ' ice scour model

  - the dimensions of the frontal mound and side berms are constant, and
  - the horizontal and vertical reaction forces between the scouring berg and the soil are constant.

- The scouring berg is assumed to be rectangular parallelopiped in shape with a front scouring face that may vary in slope, or "rake angle", within the range of $90° \leq \alpha < 180°$.

- The soil displaced by scouring is assumed to create a mound in front of the scouring berg. The frontal mound attains a steady state height, κD, and slope angle, β. Thereafter, any additional scoured soil is cleared to the sides of the scouring berg.

- A dead wedge is assumed to be created at the front face of the scouring berg. The wedge angle, ω, is determined as recommended by Been et al (1990b) with the following values for scours in sand:

Rake Angle, α	Wedge Angle, ω
90°	$90° - \phi$
120°	$90° - \phi/2$
150°	90°

The wedge angle is taken to be 90° for clay. These wedge angles are in general agreement with observations from physical model tests carried out in a centrifuge by C-CORE for the Pressure Ridge Ice Scour Experiment (PRISE). See C-CORE (1995a to i), Winsor et al (1996), Winsor and O'Neil (1996a,b,c), and Winsor and Parsons (1997a,b,c,d,e).

A passive pressure rupture zone is assumed to occur in front of the dead wedge during steady state scour conditions. The passive pressure coefficient, Kp, is determined using a log sandwich mechanism developed by Rosenfarb and Chen (1972), which compares favorably with the Sokolovsky (1965) solution.

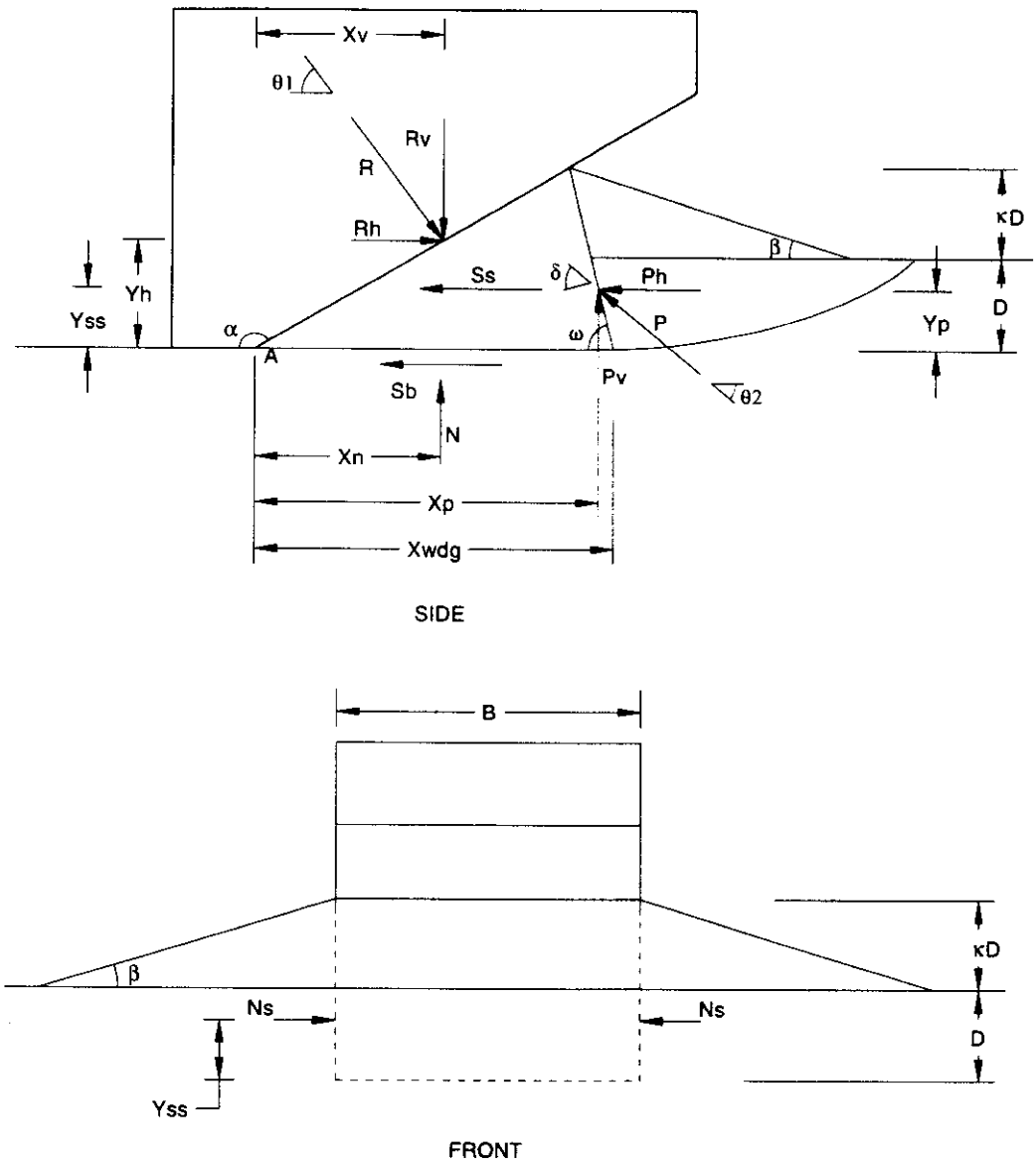

Figure 11. Scour geometry and location of scour forces

For a rough interface (i.e. $\delta = \phi$) in cohesionless soil (c'=0), the passive pressure coefficient is determined using the following expression developed by Chen and Rosenfarb (1973) which was

determined by equating the rate of external work with the rate of internal energy dissipation:

$$K_{p\gamma} = \frac{\sec\delta}{\sin\alpha + \tan\delta\cos\alpha}\left\{\frac{\sin^2\rho\cos(\rho-\phi)\cos(\alpha-\rho)\sin(\alpha+\phi)}{\sin^2\alpha\cos\phi\cos(\rho+\phi)}\right.$$
$$+\frac{\cos^2(\rho-\phi)\sin(\alpha+\phi)}{\sin^2\alpha\cos^2\phi\,(1+9\tan^2\phi)\cos(\rho+\phi)}[\cos(\alpha-\rho)[-3\tan\phi+(3\tan\phi\cos\psi+\sin\psi)$$
$$\times\exp(3\psi\tan\phi)]+\sin(\alpha-\rho)[1+(3\tan\phi\sin\psi-\cos\psi)\exp(3\psi\tan\phi)]]$$
$$\left.+\frac{\cos^2(\rho-\phi)\sin(\alpha-\rho-\psi+\beta)\cos(\alpha-\rho-\psi)\sin(\alpha+\phi)\exp(3\psi\tan\phi)}{\sin^2\alpha\cos\phi\cos(\alpha-\rho-\psi+\beta+\phi)\cos(\rho+\phi)}\right\}$$

For a smooth interface (i.e. $\delta < \phi$) in cohesionless soil (c'=0), the passive pressure coefficient is determined using:

$$K_{p\gamma} = \frac{\sec\delta}{\sin\alpha+\tan\delta\cos\alpha-\dfrac{\tan\delta\cos(\alpha-\rho)}{\cos\rho}}\left\{\frac{\tan\rho\cos(\rho-\phi)\cos(\alpha-\rho)}{\sin\alpha\cos\phi}\right.$$
$$+\frac{\cos^2(\rho-\phi)}{\cos\rho\sin\alpha\cos^2\phi(1+9\tan^2\phi)}[\cos(\alpha-\rho)[-3\tan\phi\cos\psi+\sin\psi)$$
$$\times\exp(3\psi\tan\phi)]+\sin(\alpha-\rho)[1+(3\tan\phi\sin\psi-\cos\psi)\exp(3\psi\tan\phi)]]$$
$$\left.+\frac{\cos^2(\rho-\phi)\sin(\alpha-\rho-\psi+\beta)\cos(\alpha-\rho-\psi)\exp(3\psi\tan\phi)}{\cos\phi\sin\alpha\cos(\alpha-\rho-\psi+\phi+\beta)\cos\rho}\right\}$$

In a cohesive soil (c'>0) with a smooth interface ($\delta < \phi$), the passive pressure coefficient is determined using:

$$K_{pc} = \frac{\sec\alpha}{\sin\alpha+\tan\delta c\cos\alpha}\times\left\{\frac{\cos\phi\cos(\alpha-\rho)}{\sin\alpha\cos(\rho+\phi)}+\frac{\sin\rho\sin(\alpha+\phi)}{\sin\alpha\cos(\rho+\phi)}\right.$$
$$+\frac{\cos(\rho-\phi)\sin(\alpha-\rho-\psi+\beta)\sin(\alpha+\phi)\exp(2\psi\tan\phi)}{\sin\alpha\cos(\alpha-\rho-\psi+\phi+\beta)\cos(\rho+\phi)}$$
$$\left.+\frac{\cos(\rho-\phi)\sin(\alpha+\phi)[\exp(2\psi\tan\phi)-1]}{\sin\phi\sin\alpha\cos(\rho+\phi)}\right\}$$

In a cohesive soil (c'>0) with a rough interface ($\delta = \phi$), the passive pressure coefficient is determined using:

$$K_{pc} = \frac{\sec\alpha}{\sin\alpha + \tan\delta\cos\alpha - \dfrac{\tan\delta\cos(\alpha-\rho)}{\cos\rho}} \times \left\{ \tan\rho + \frac{\cos(\rho-\phi)\sin(\alpha-\rho-\psi+\beta)\exp(2\psi\tan\phi)}{\cos\rho\cos(\alpha-\rho-\psi+\phi+\beta)} + \frac{\cos(\rho-\phi)[\exp(2\psi\tan\phi)-1]}{\sin\phi\cos\rho} \right\}$$

The above passive pressure coefficient equations are solved using an iterative procedure where ρ and ψ are varied to obtain a minimum value for Kp. The passive pressure coefficients are determined separately for the cohesion and friction components and the results are superimposed to determine the overall passive pressure.

- A correction factor, K_{3D}, is applied to the computed passive pressure force acting at the front of the scour to account for the rupture zone extending to the sides of the scour (see Figures 12 and 13).

  $K_{3D} = 1 + \pi D/[6B \tan(45-\phi/2)]$

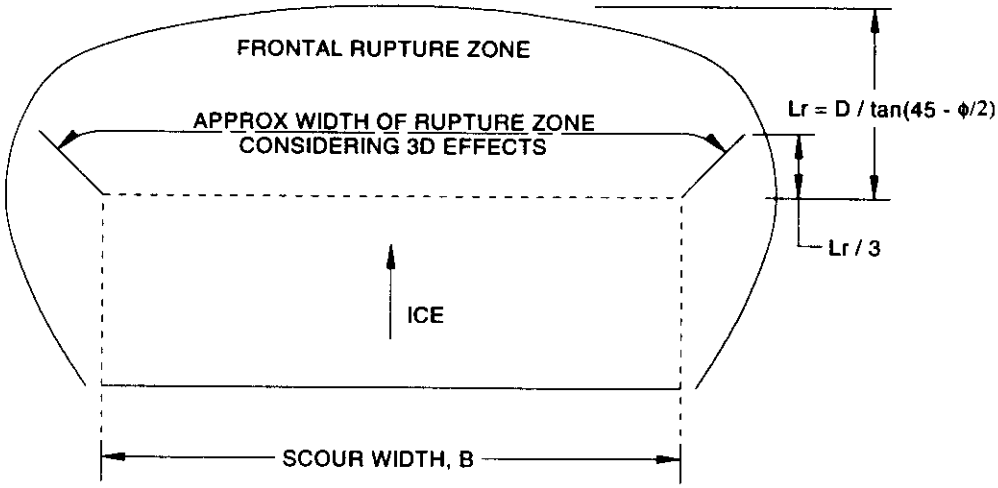

Figure 12. Scour width correction to account for 3D effects

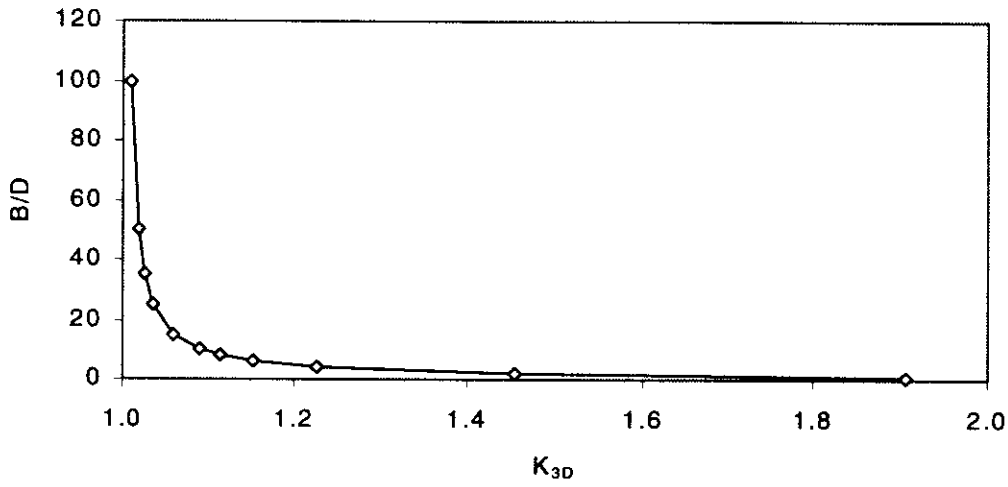

Figure 13. Variation of passive pressure correction factor with B/D ratio

– The passive pressure forces are determined as:

$P_1 = \frac{1}{2}\gamma' B(D+\kappa D)^2 K_{3D} K_{p\gamma}$ (frictional component)

$P_2 = 2\, c'\, B\, D\, K_{3D} K_{pc}^{\frac{1}{2}}$ (cohesive component)

$P = P_1 + P_2$

These forces are assumed to act on the front face of the dead wedge at heights of Y_{p1} and Y_{p2} above the base of the scour.

$Y_{p1} = (D+\kappa D) / 3$ (frictional component)

$Y_{p2} = D/2$ (cohesive component)

$Y_p = (P_1 Y_{p1} + P_2 Y_{p2}) / (P_1 + P_2)$

The passive resistance force acts at an angle of $\theta_2 = \omega + \delta - 90°$ from the horizontal.

- Side shear resistance, Ss, is generated on both sides of the dead wedge. The side shear resistance is determined for each side of the wedge as:

$S_{s1} = \frac{1}{2} \gamma' (D+\kappa D) f_s K_{p\gamma} A_{wdg} \tan\phi_{cv}$ (frictional component)

$S_{s2} = c' A_{wdg}$ (cohesive component)

$S_s = S_{s1} + S_{s2}$

A_{wdg} is the area of the dead wedge over which shearing occurs and f_s is a passive pressure reduction factor to account for a lower Kp at the sides of the scour than at the front of the scour. The friction angle used for determining the shear resistance is the large strain (constant volume) friction angle.

- Base shear resistance, Sb, is generated along the bottom of the dead wedge.

$Sb = N \tan\phi_{cv}$

where N is the vertical load acting on the soil and ϕ_{cv} is the large strain friction angle of the soil.

3.3 Determination of Soil Reaction Force and Point of Application

The soil reaction due to ice scour is determined by resolving forces in the horizontal and vertical directions.

a) Force equilibrium in the horizontal direction: $R \cos\theta_1 = 2Ss + N \tan\phi + Ph$

b) Force equilibrium in the vertical direction: $R \sin\theta_1 = N + Pv$

If it is assumed that the orientation of the resultant force is known, $\theta_1 \approx 45°$ based on PRISE ice scour experiments carried out by C-CORE (C-CORE 1995a to i; Winsor et al 1996; Winsor and O'Neil 1996a,b,c; Winsor and Parsons 1997a, b,c,d,e), the magnitude of the resultant is,

$$R = (Ph + 2Ss - Pv \tan\phi) / (\cos\theta_1 - \sin\theta_1 \tan\phi)$$

with a horizontal component of, $Rh = R \cos\theta_1$

and a vertical component of, $Rv = R \sin\theta_1$

The magnitude of the normal force is, $N = R \sin\theta_1 - Pv$

The location of the resultant force with respect to the scouring berg is determined from moment equilibrium which gives:

$$Xv = [(Nxn + 2SsYss + PhYp + PvXp)/R] [\cos(180-\alpha)/\sin(180-\alpha+\theta_1)]$$

$$Yh = [(Nxn + 2SsYss + PhYp + PvXp)/R] [\sin(180-\alpha)/\sin(180-\alpha+\theta_1)]$$

Table 5. Summary of abbreviations and symbols used in C-CORE model

Parameter		Description
R	=	soil reaction force
Rh	=	horizontal component of soil reaction force
Rv	=	vertical component of soil reaction force
P	=	passive resistance force
Ph	=	horizontal component of passive resistance force
Pv	=	vertical component of passive resistance force
N	=	normal force on bottom of dead wedge
Sb	=	shear force on bottom of dead wedge
Ss	=	shear force on sides of dead wedge
Ns	=	normal force on sides of dead wedge
Kp	=	passive pressure
K_{3D}	=	passive pressure correction factor for 3D effects
f_s	=	passive pressure reduction factor for side shear
Xv	=	horiz distance from base of scour to point at which reaction force acts
Yh	=	height at which horizontal component of reaction force acts
Yp	=	height at which horizontal component of passive pressure acts
Xp	=	horiz distance from base of scour to point at which passive force acts
Xn	=	horiz distance from base of scour to point at which normal force acts
Yss	=	height at which side shear force acts above base of scour
D	=	scour depth below original sea floor elevation
κD	=	height of frontal mound
Xwdg	=	width of dead wedge
α	=	rake angle
θ_1	=	angle of resultant soil reaction force with respect to horizontal
θ_2	=	angle of passive pressure force with respect to horizontal
δ	=	wall friction angle
β	=	slope angle of frontal mound
ω	=	wedge angle
γ'	=	effective (buoyant) unit weight of the soil
ϕ'	=	effective friction angle of the soil

4.0 C-CORE MODEL FOR UNDRAINED SCOURING

4.1 Model Description

The C-CORE undrained scour model assumes steady state scouring where the scour force, the scour depth, the scour width, and the size of the frontal mound and side berms remain constant over large scour distances (often in the order of 1000's of metres in length). In the model, a virtual work calculation is carried out based on an assumed incremental mechanism. The horizontal scour resistance is calculated by balancing the work input to the system with the energy dissipated from the system. Several mechanisms are considered in the analysis including:

- shear resistance along the base of a dead wedge created in front of the scouring berg,
- shear resistance along the base of a passive wedge created in front of the dead wedge,
- shear resistance along the interface between the dead and passive wedges,
- shear resistance on the two sides of the dead and passive wedges, and
- a clearing mechanism for moving accumulated soil to the sides of the berg during scouring.

These mechanisms are shown schematically in Figure 14. The vertical scour resistance is limited by the vertical bearing capacity of the soil under the dead wedge. The model does not take into account the energy required to shear the soil as the direction of soil movement changes (a soil particle in the centre of the scour path initially moves parallel to the ice movement and as displacement increases, the soil particle movement becomes perpendicular to the ice movement direction). The geometric distortion and the restraint of the keel above the soil are not considered in the model.

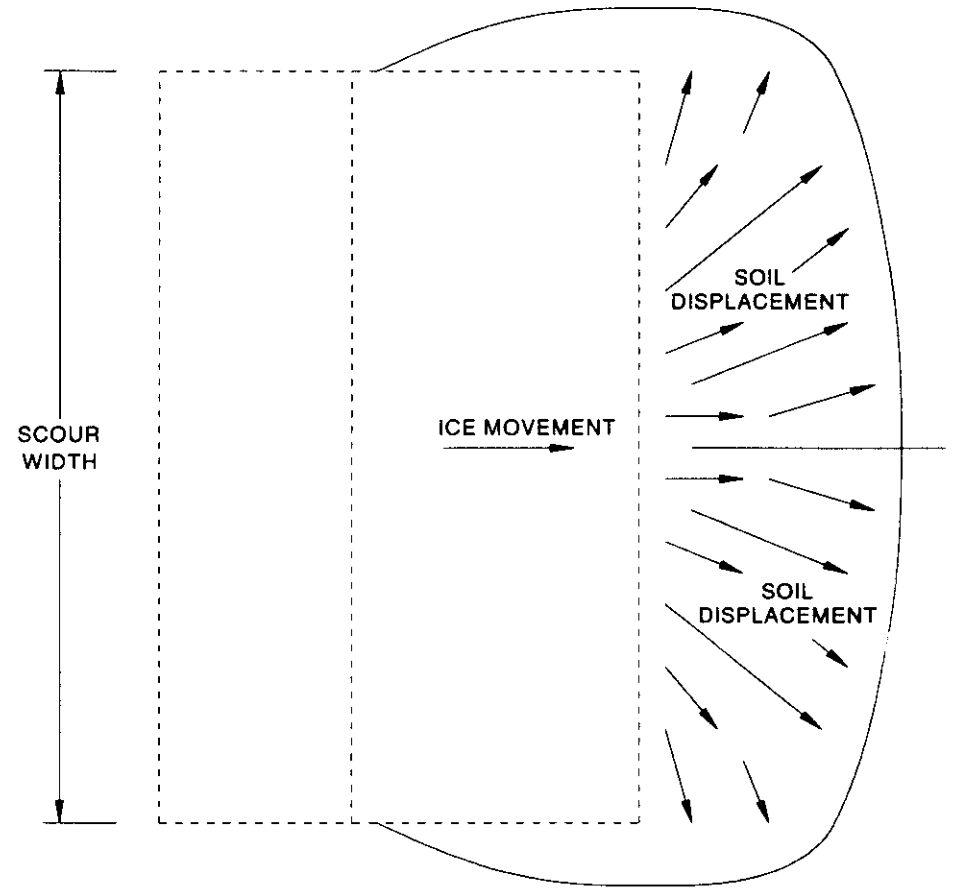

Figure 14. Mechanism for undrained ice scour model

4.2 Formulation of Ice Scour Model

The assumed scour geometry and the location of the forces are shown on Figure 15 and Figure 16. The horizontal and vertical scouring forces are designated by R_h and R_v. Soil resistance forces along the base of the dead wedge, the dead/passive wedge interface, the base of the passive wedge, the sides of the dead wedge, and the sides of the passive wedge are designated R1, R2, R3, R4, and R5, respectively. The weight of the passive soil block, the surcharge, and the soil cleared to the sides of the scouring berg are designated W1, W2 and W3, respectively. The magnitude, location, and orientation of the resultant soil reaction forces, R_h and R_v, can be determined using the scour model developed on the following pages. A summary of symbols and abbreviations used in formulating the scour model is presented in Table 7 located at the end of section 4.

The methodology and assumptions used in formulating the scour model are summarized as follows:

- The soil is cohesive and scouring is sufficiently rapid that no dissipation of pore pressure occurs during scouring,

- The base of the scour is parallel with the sea floor (this is equivalent to assuming that the sea floor is horizontal and the scour depth is constant).

- Steady state scouring conditions are assumed where:
  - scour depth, D, is constant,
  - scour width, B, is constant,
  - the dimensions of the frontal mound and side berms are constant, and
  - horizontal and vertical reaction forces between the ice and the soil are constant.

- The scouring berg is assumed to be rectangular parallelopiped in shape with a front scouring face that may vary in slope, or "rake angle", within the range of $90° \leq \alpha < 180°$.

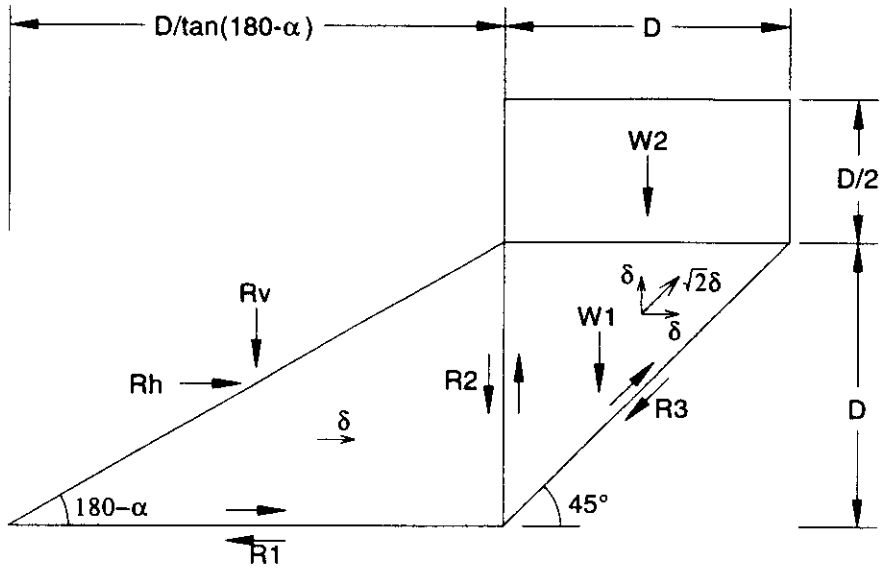

Figure 15. Forces considered in analysis (in cross-section)

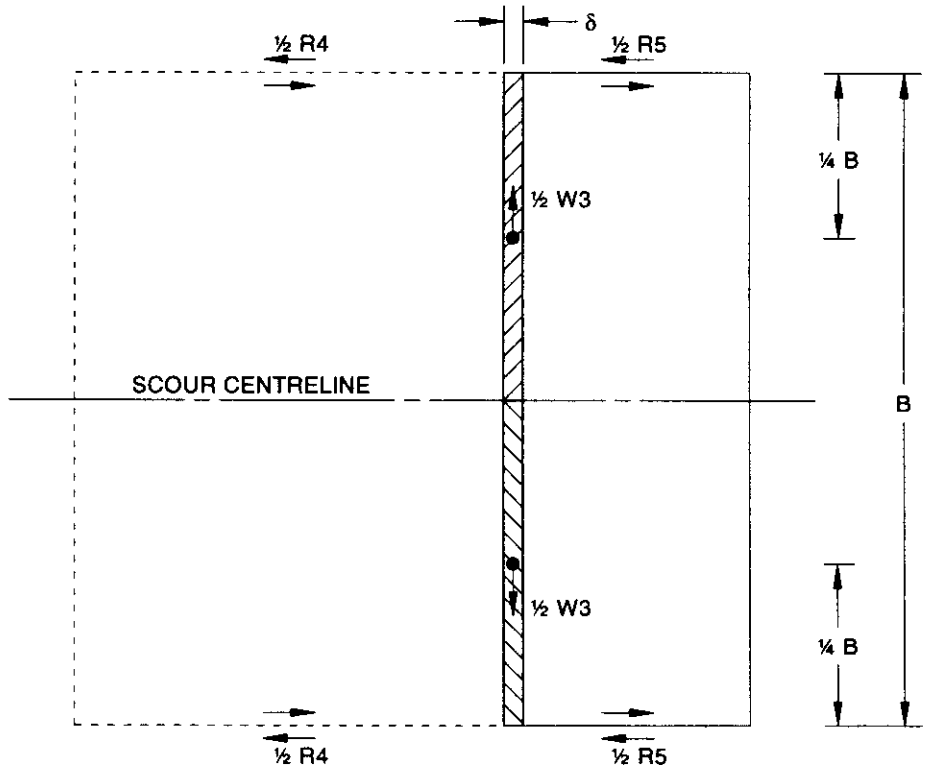

Figure 16. Forces considered in analysis (in plan)

- The soil displaced by scouring is assumed to create a mound in front of the scouring berg. The frontal mound is assumed to attain a steady state height, κD such that the height of an equivalent rectangular surcharge is equal to ½D. Thereafter, any additional scoured soil is cleared to the sides of the scouring berg.

- A dead wedge is assumed to be created at the front face of the scouring berg. The wedge angle is taken to be 90° for clay.

- A passive pressure rupture zone is assumed to occur in front of the dead wedge during steady state scour conditions. The slope of the rupture surface from the horizontal is taken as 45°.

Consider the work carried out by moving an ice feature a horizontal distance of δ, while the soil is being scoured to a depth D. It is assumed that the vertical displacement of the ice is zero during scouring. The work into the system and the energy dissipated during scour are determined as shown in Table 6. From these relationships, the normalized horizontal scouring force is determined as:

$$\frac{R_h}{C_u DB} = \frac{1}{\tan(180-\alpha)} + 1 + 2 + \frac{D}{B\tan(180-\alpha)} + \frac{\sqrt{2}D}{B} + \frac{\gamma' D}{C_u} + \frac{\gamma' B}{4C_u}$$

with the horizontal soil resistance being

$$R_h = C_u DB\left[\frac{1}{\tan(180-\alpha)} + 1 + 2 + \frac{D}{B\tan(180-\alpha)} + \frac{\sqrt{2}D}{B} + \frac{\gamma' D}{C_u} + \frac{\gamma' B}{4C_u}\right]$$

The vertical scour resistance is assumed to be limited by the vertical bearing capacity of the soil which is determined using the following relation.

$$R_v \le [5.14C_u + 1.5D(\gamma' + \gamma_w)]X_{wdg}B \times \left(1 - \frac{\lambda}{90°}\right)^2$$

Table 6. Development of a relation for the overall horizontal scour resistance

Term	Displ.	Force	Work	Force Term Description
Work In				
R_h	δ	R_h	δR_h	Total horizontal force applied to soil
R_v	0	R_v	0	Total vertical force applied to soil
Energy Out				
R1	δ	$C_uBD/\tan(180-\alpha)$	$\delta C_uBD/\tan(180-\alpha)$	Soil resistance along base of dead wedge
R2	δ	C_uBD	δC_uBD	Soil resistance on dead/passive wedge interface
R3	$\sqrt{2}\,\delta$	$\sqrt{2}\,C_uBD$	$2\delta C_uBD$	Soil resistance along base of passive wedge
R4	δ	$C_uD^2/\tan(180-\alpha)$	$\delta C_uD^2/\tan(180-\alpha)$	Soil resistance along sides of dead wedge
R5	$\sqrt{2}\,\delta$	C_uD^2	$\sqrt{2}\,\delta C_uD^2$	Soil resistance along sides of passive wedge
W1	δ	$\frac{1}{2}\gamma' D^2B$	$\frac{1}{2}\delta\gamma' D^2B$	Force required to lift passive wedge
W2	δ	$\frac{1}{2}\gamma' D^2B$	$\frac{1}{2}\delta\gamma' D^2B$	Force required to lift frontal mound
W3	$\frac{1}{4}B$	$\delta\gamma' DB$	$\frac{1}{4}\delta\gamma' DB^2$	Force to clear soil to sides of scouring berg

Table 7. Summary of abbreviations and symbols used in C-CORE model

Term	Description
B =	scour width
D =	scour depth below original sea floor elevation
0.5D=	height of equivalent surcharge due to frontal mound development
α =	rake angle
ω =	wedge angle
C_u =	undrained strength of cohesive soil
γ' =	effective (buoyant) unit weight of the soil
γ_w =	unit weight of water
R_h =	horizontal component of soil reaction force
R_v =	vertical component of soil reaction force
R1 =	shear resistance developed on bottom of dead wedge
R2 =	soil resistance on dead/passive wedge interface
R3 =	soil resistance along base of passive wedge
R4 =	soil resistance along sides of dead wedge
R5 =	soil resistance along sides of passive wedge
W1=	force required to lift passive wedge
W2=	force required to lift surcharge soil
W3=	force to clear soil to sides of scouring berg
X_{wdg}=	length of dead wedge
δ =	incremental displacement used in work/energy calculations
λ =	angle of resultant force from vertical (assume maximum λ=30°)

5.0 COMPARISON OF ICE SCOUR MODELS

5.1 Ice Scouring With Drained Conditions

5.1.1 Comparison with test data and other models

Scour forces computed using the Surkov model, the Been model, and the C-CORE c-ϕ' model are shown in Figure 17. Scour forces determined from PRISE tests in sand are compared in Figure 18 with scour forces calculated using the C-CORE model. Parameters used in these analyses are summarised in Table 8.

The Chari model was developed for analysing scours in cohesive soils and cannot be readily applied to granular materials. The Kioka model uses rather complex mathematics and scour path trajectory for calculating scour forces, and was not compared to the other models or to the PRISE data.

In the formulation of the Surkov model, it was assumed that all of the displaced soil remains at the front of the scouring berg and contributes to the passive resistance of the frontal wedge. For scours in short steep slopes, smaller volumes of soil will be accumulated for larger scour depths and the use of the Surkov model may give results that are comparable to those generated using the C-CORE model. For long scour lengths where the sea bottom is horizontal or nearly horizontal, the Surkov model will indicate a tremendous volume of soil retained in front of the ice feature and very large scour forces will be computed.

The Been model was originally formulated to consider the normal force and shear resistance at the bottom of the ice in addition to the horizontal and vertical components of passive resistance. The computer program provided (Been et al 1990b), however, has not been developed to the stage where a base resistance component is included in the scour resistance calculations. The scour forces calculated are based solely on the horizontal and vertical components of passive resistance.

Scour forces calculated using the C-CORE model with effective friction angles of 35° and 40° provide approximate upper and lower limits to the forces observed during the PRISE tests in sand and are shown in dimensionless form in Figure 18.

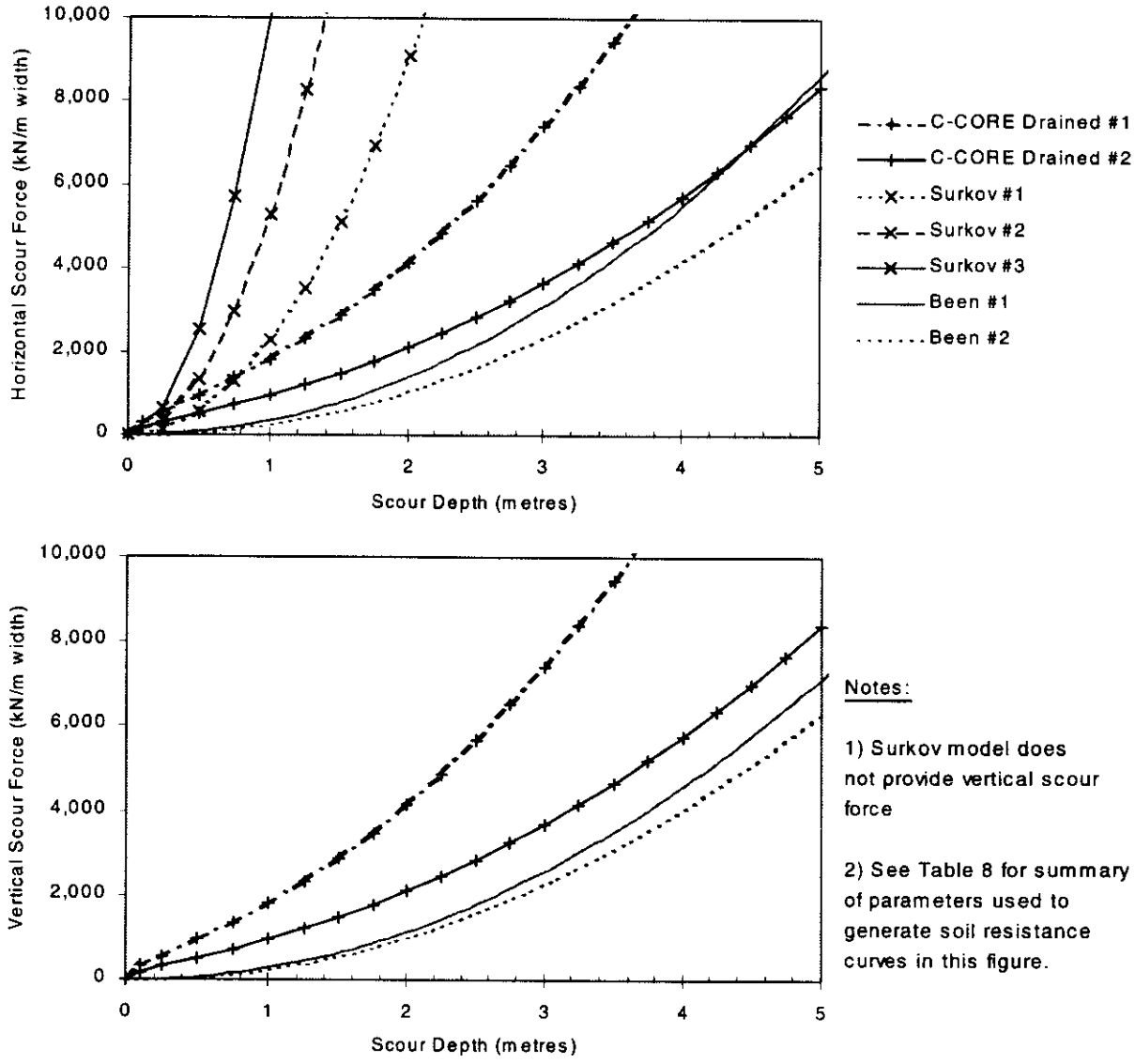

Figure 17. Comparison of scour models for drained conditions

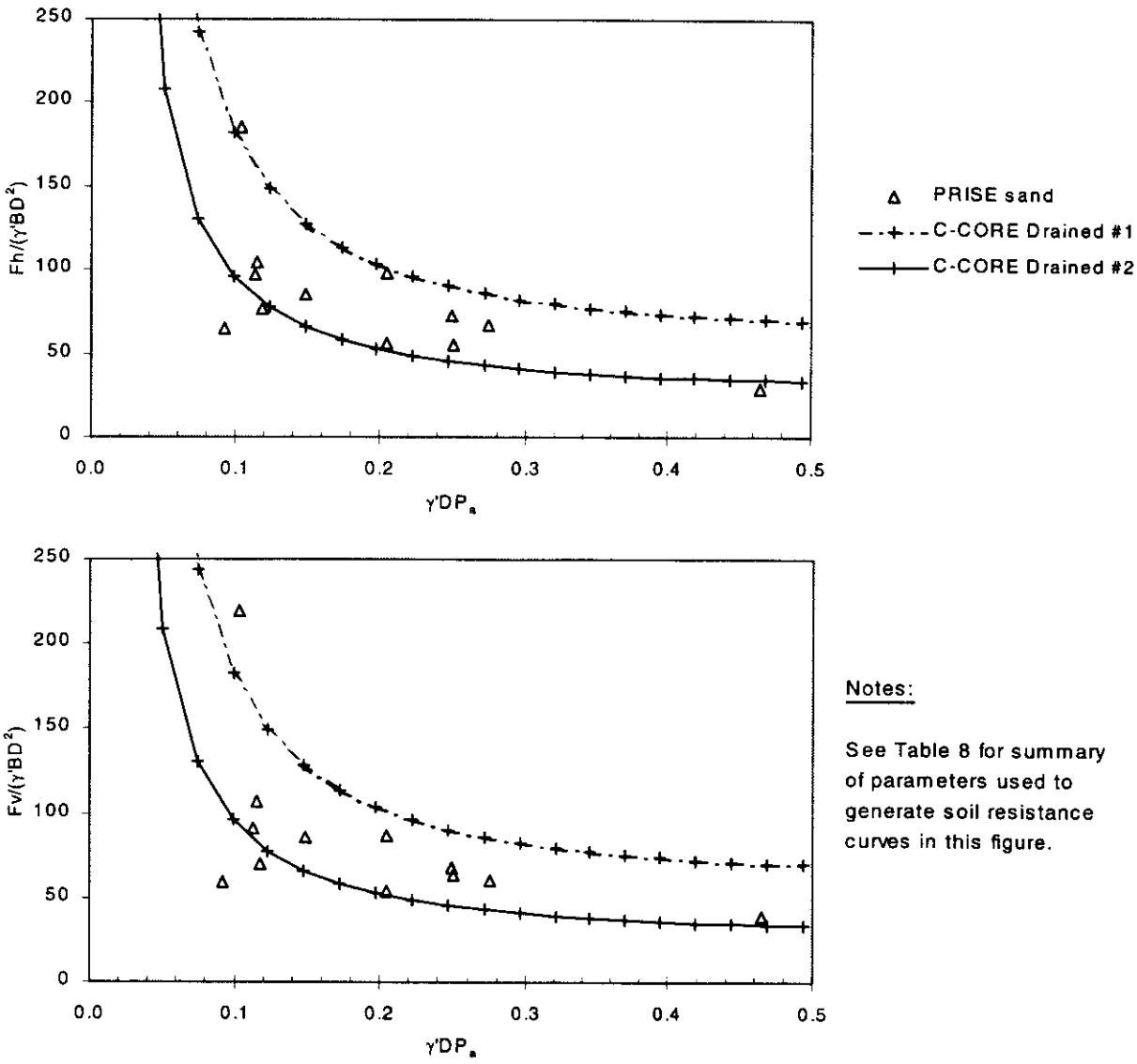

Figure 18. Comparison of C-CORE drained scour model with test data

Table 8. Parameters used for scour calculations shown in Figures 17 and 18

Parameter		Surkov Model			Been Model		C-CORE Drained Model	
		#1	#2	#3	#1	#2	#1	#2
γ'	kN/m^3	10	10	10	10	10	10	10
ϕ'	deg	35	35	35	40	35	40	35
ϕ_{cv}'	deg	35	35	35	37	32	37	32
c'	kPa	-	-	-	0	0	0	0
rake angle	deg	90	90	90	165	165	165	165
scour width	m	-	-	-	-	-	15	15
bed slope		1:200	1:500	1:1000	1:1500	1:1500	horizontal	horizontal
surcharge	kPa/m	-	-	-	10	10	~10	~10
atm pressure	kPa	101.3	101.3	101.3	101.3	101.3	101.3	101.3

5.1.2 Sensitivity of model to variations in parameters

A sensitivity analysis was carried out to demonstrate how scour forces computed using the C-CORE drained model will vary with changes to key parameters. The results of the sensitivity analysis are presented in Figures 19 through 23.

In Figure 19, the horizontal scour force per unit scour width is plotted versus depth for scour widths of 15 m, 20 m, 25 m and 30 m. Although there is a reduction in scour force due to the reduced three dimensional effects as the scour width increases; the observed increase in scour force with increasing scour width is primarily due to the height of the surcharge increasing as the ratio of scour width to scour depth increases.

Figure 20 shows a decrease in the scour resistance with decreasing frictional strength which is expected for the assumed scour mechanism. The scour resistance is relatively insensitive to moderate changes in effective cohesion, as is indicated in Figure 21.

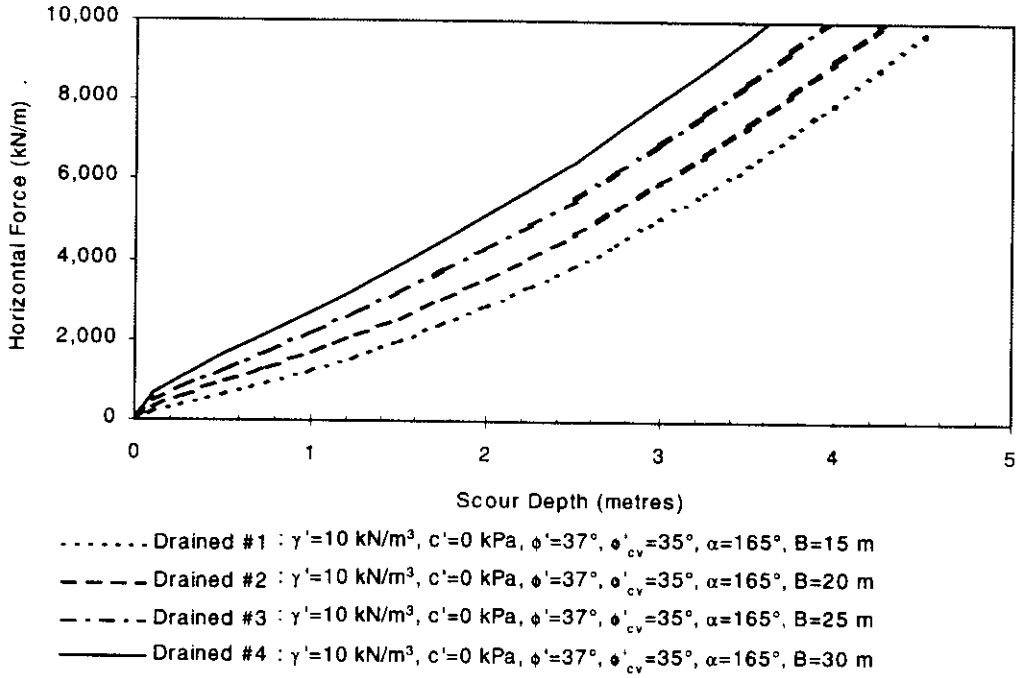

Figure 19. Sensitivity of drained model to B

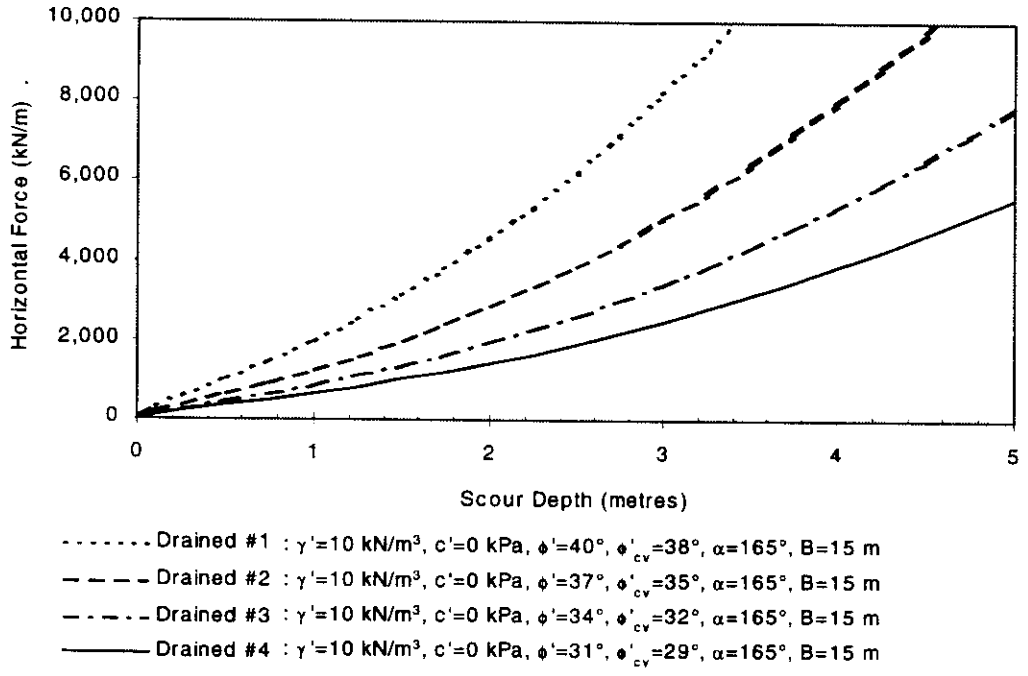

Figure 20. Sensitivity of drained model to ϕ'

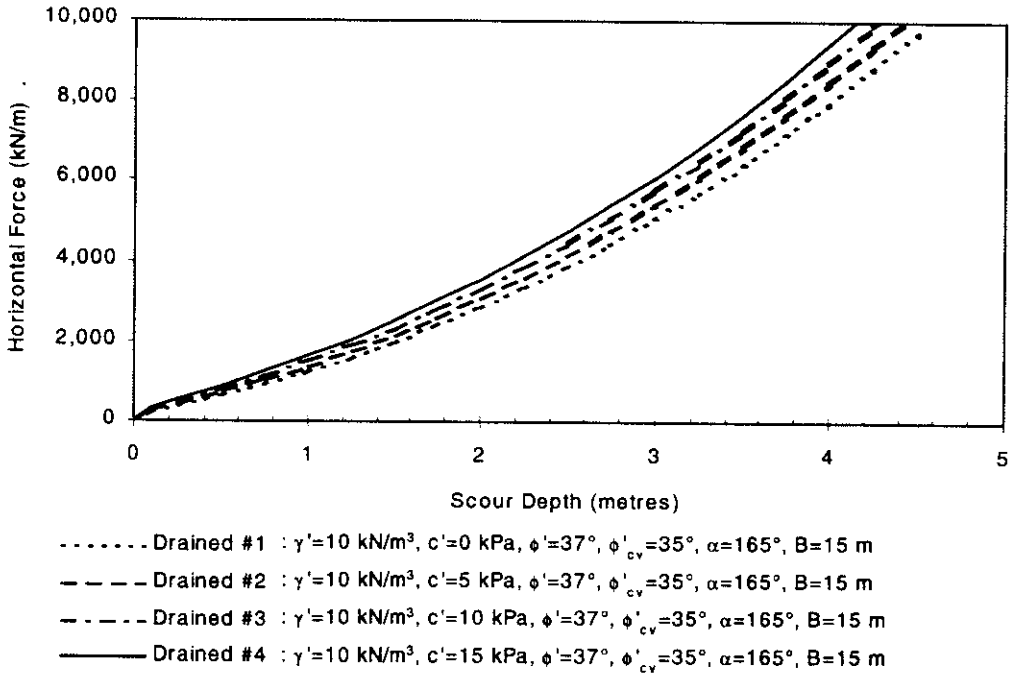

Figure 21. Sensitivity of drained model to c'

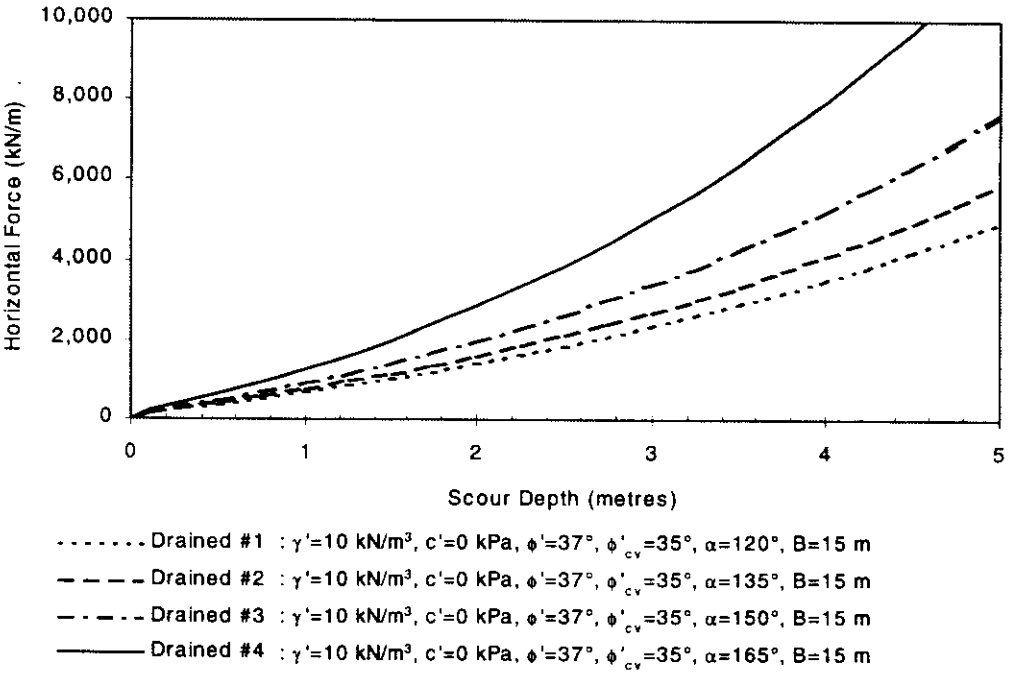

Figure 22. Sensitivity of drained model to α

Figure 22 indicates there is a significant increase in scour resistance as the rake angle is increased from 120 to 165 degrees. This trend is in agreement with the results of the PRISE tests on sand.

As shown in Figure 23, the effect of increasing the effective unit weight of soil from 6 to 12 kN/m^3, is a substantial increase in the scour force.

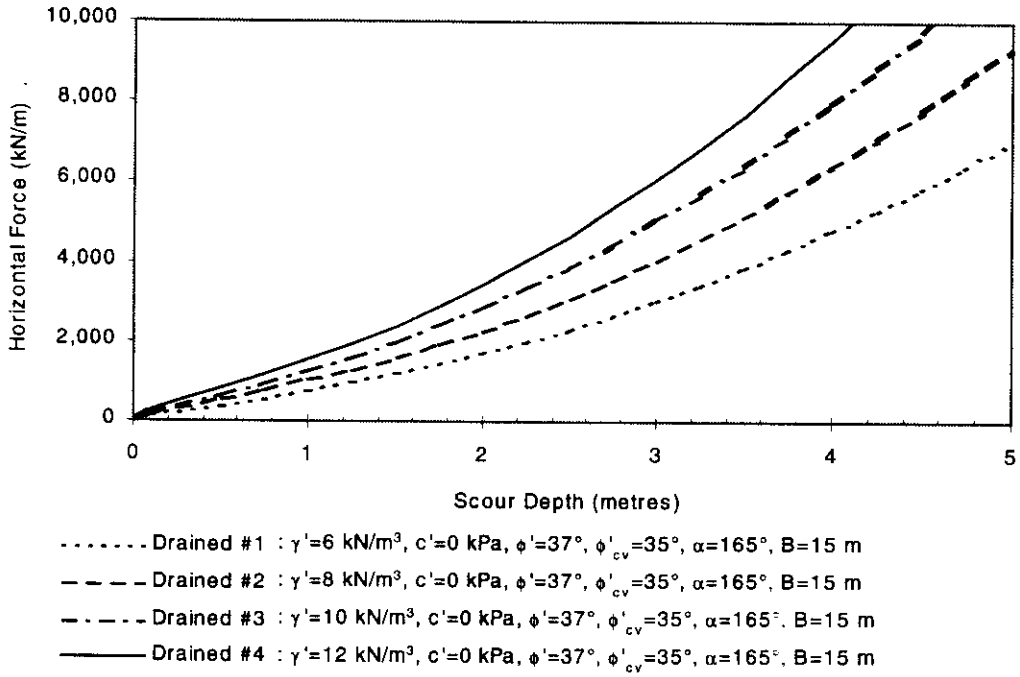

Figure 23. Sensitivity of drained model to γ'

5.2 Ice Scouring With Undrained Conditions

5.2.1 Comparison with test data and other models

The soil resistance determined using the Chari and the C-CORE undrained models are plotted in Figure 24. The horizontal scour forces calculated using the C-CORE model are substantially greater than those calculated using the Chari model with the same soil conditions. The vertical scouring force is not determined using the Chari model.

In Figure 25, the horizontal and vertical scour forces determined using the C-CORE undrained and drained models are plotted in a dimensionless form together with results from PRISE tests in silty clay and results of tests carried out by Lach (1996) in Speswhite kaolin clay.

The PRISE and Lach (1996) tests had relatively shallow model scours and there was some excess pore pressure dissipation during the scour events. These test results should therefore be bracketed by the undrained and drained model predictions. The PRISE tests results are comparable to the C-CORE undrained model #3 and drained model #2 predictions. The Lach (1996) results are comparable to the C-CORE undrained model #2 and drained model #1 predictions. The horizontal force results are reasonably bounded by these predictions. The kaolin test and deep scour results are close to the undrained predictions. The vertical force results are generally closer to, and distributed about, the drained model predictions.

Table 9 summarises the parameters used in calculating the forces plotted in Figures 24 and 25.

Table 9. Parameters used for scour calculations shown in Figures 24 and 25

Parameter		Chari Model				C-CORE Undrained Model				C-CORE Drained Model	
		#1	#2	#3	#4	#1	#2	#3	#4	#1	#2
γ'	kN/m^3	8	8	8	8	8	8	8	8	8	8
c_u	kPa	10	25	50	100	10	25	50	100	7	6.5
ϕ'	deg	--	--	--	--	--	--	--	--	23	30
α	deg	90	90	90	90	165	165	165	165	165	165
B	m	30	30	30	30	30	30	30	30	30	30
Pa	kPa	101.3	101.3	101.3	101.3	101.3	101.3	101.3	101.3	101.3	101.3

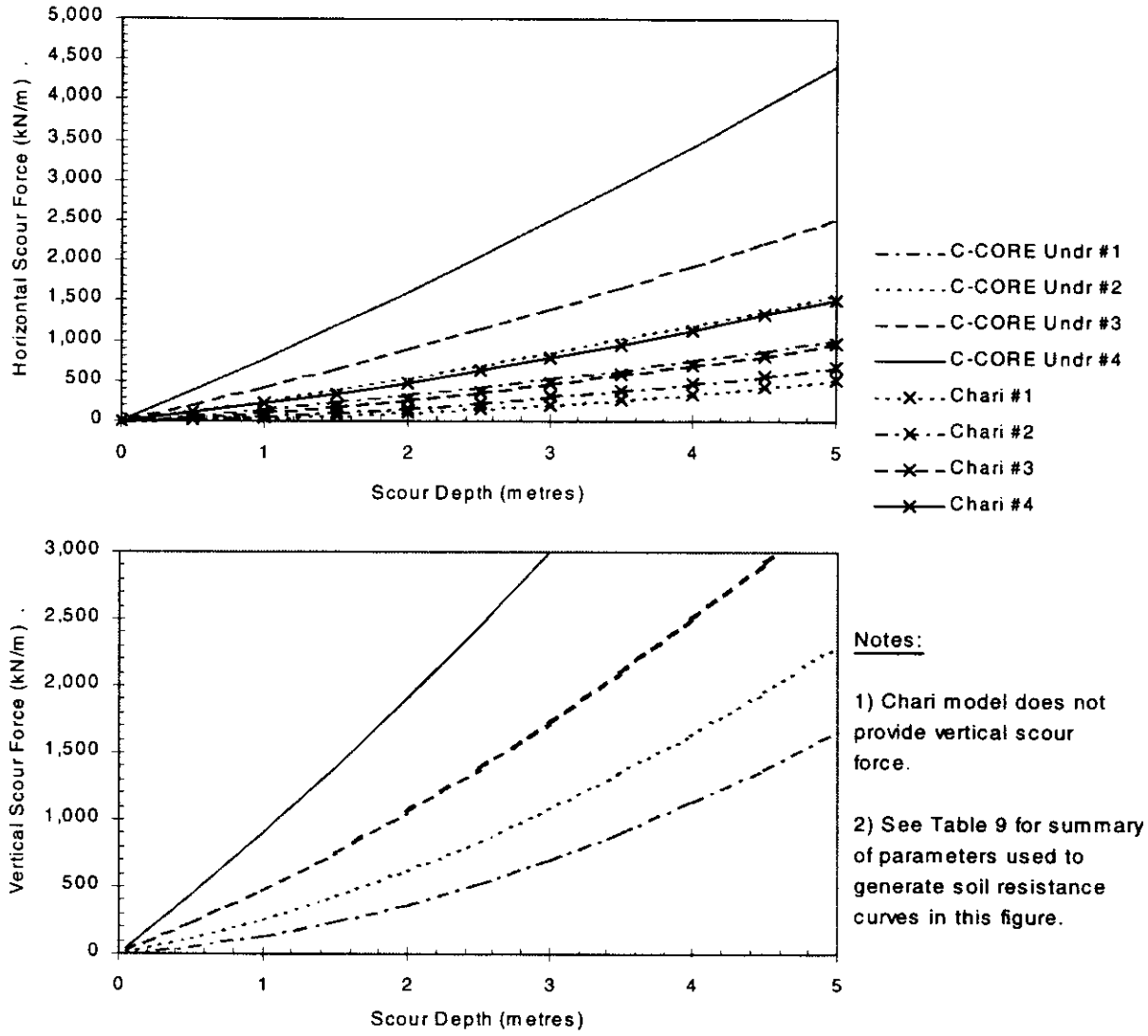

Figure 24. Comparison of Chari and C-CORE models for undrained conditions

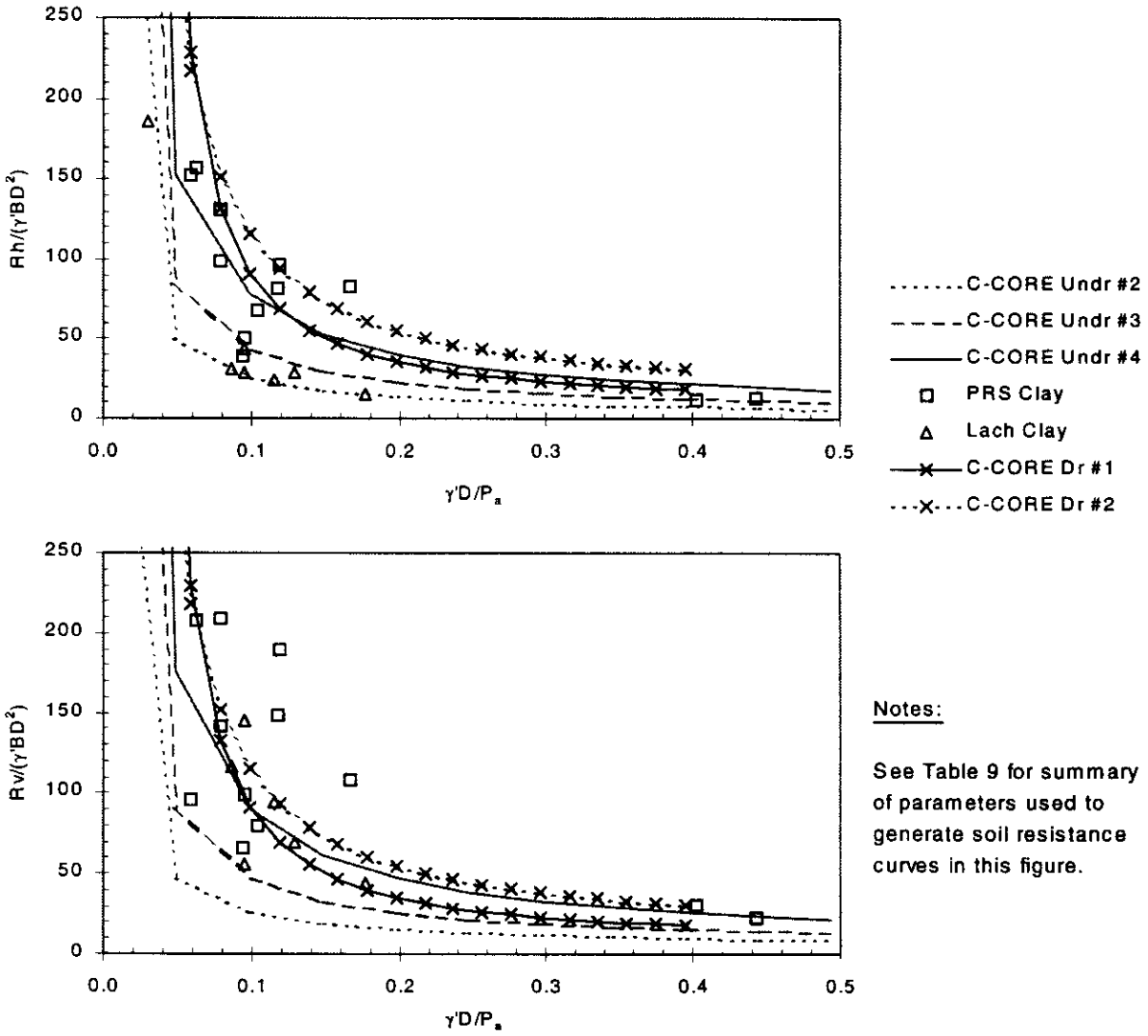

Figure 25. Comparison of test data to drained and undrained models

5.2.2 Sensitivity of model to variations in parameters

A sensitivity analysis was carried out to determine how scour forces computed using the C-CORE undrained model will vary with changes to key parameters. The results of the sensitivity analysis are presented in Figures 26 through 29.

Figure 26 indicates that the vertical scour force is insensitive to changes in the scour width, whereas the horizontal scour force will increase significantly for wide and deep scours.

Figure 27 indicates that both the horizontal and vertical scour resistance will vary substantially with different rake angles. This is in agreement with the results from PRISE tests where the scour resistance increases with larger rake angles.

As indicated by Figure 28, both the horizontal and vertical scour resistance will increase with increasing undrained strength. The model indicates that the ratio of the vertical to horizontal scour force is relatively constant with depth for strong soils and increases with increasing depth for weaker soil.

The scour forces are relatively insensitive to variations in the effective unit weight of the soil (Figure 29). There is a slight increase in the scour forces with increasing unit weight for deep scours.

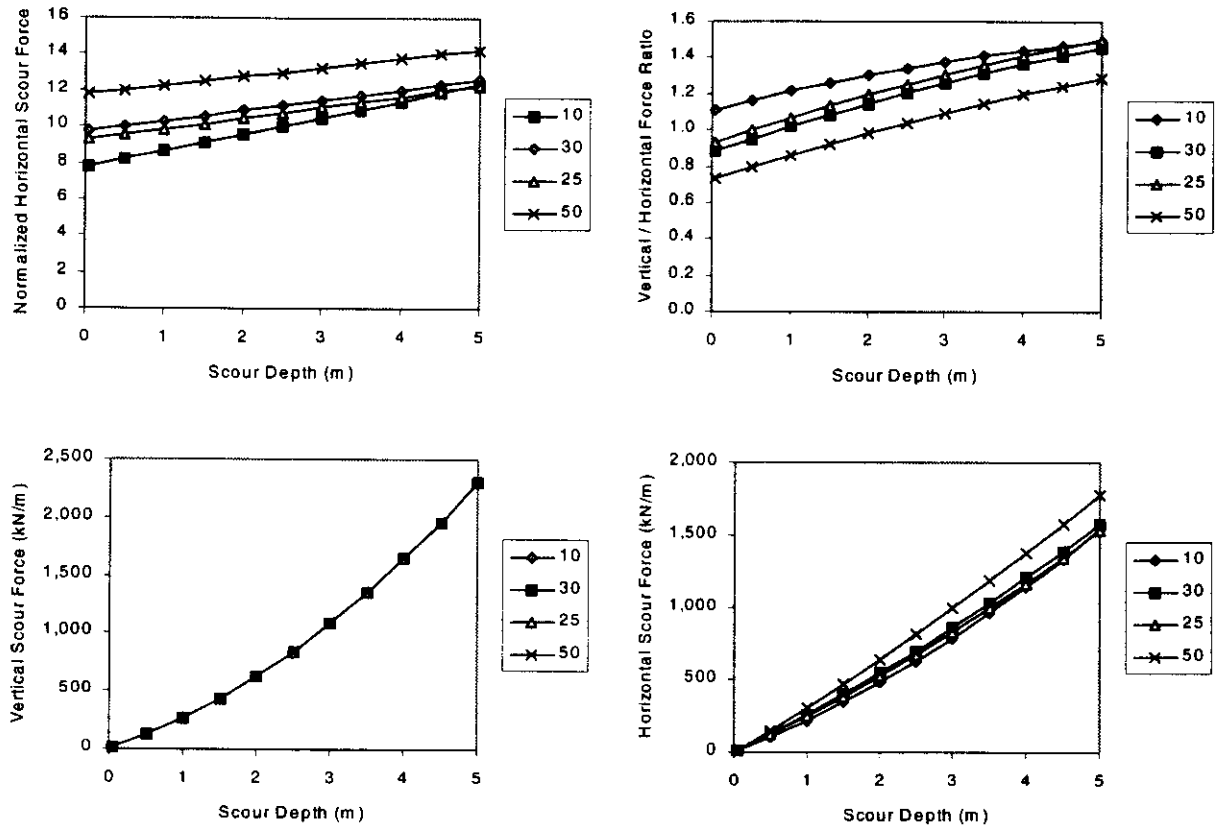

Figure 26. Sensitivity of undrained model to B (α=165°, c_u=25 kPa, γ'=10 kN/m3)

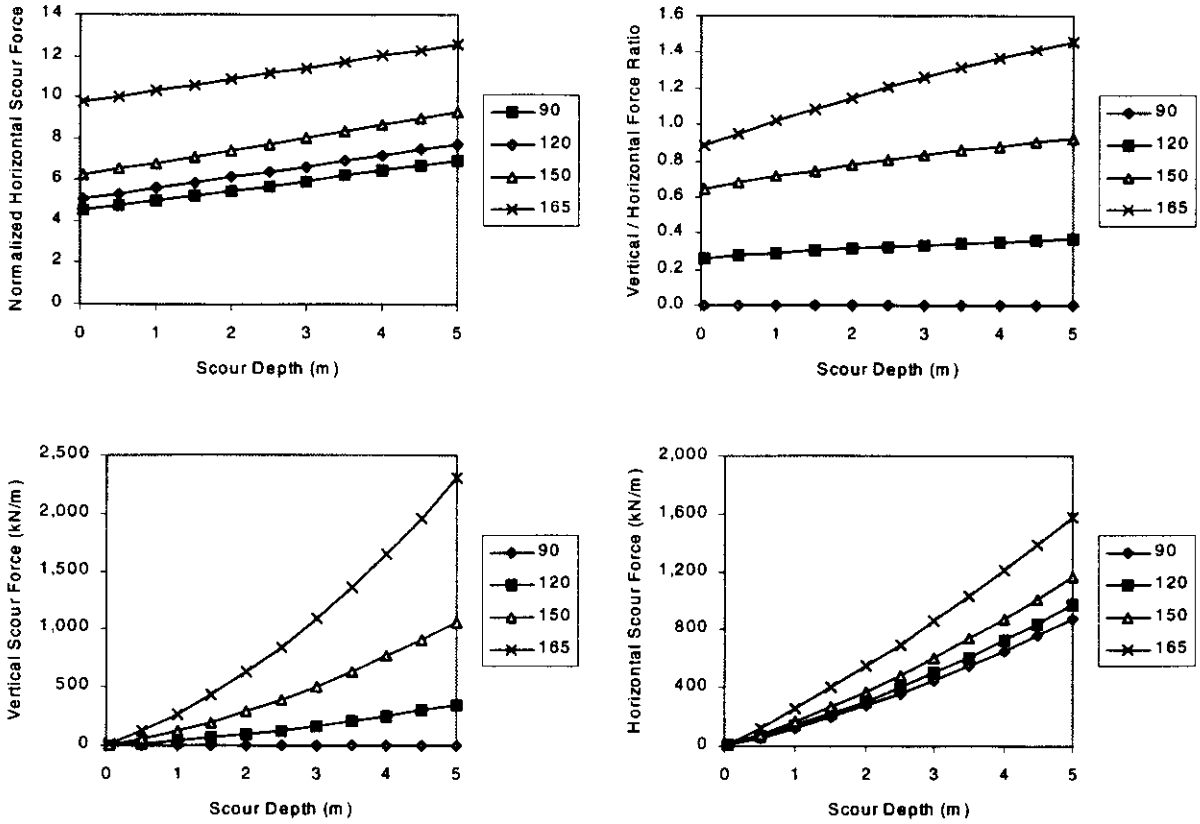

Figure 27. Sensitivity of undrained model to α (B=15 m, c_u=25 kPa, γ'=10 kN/m3)

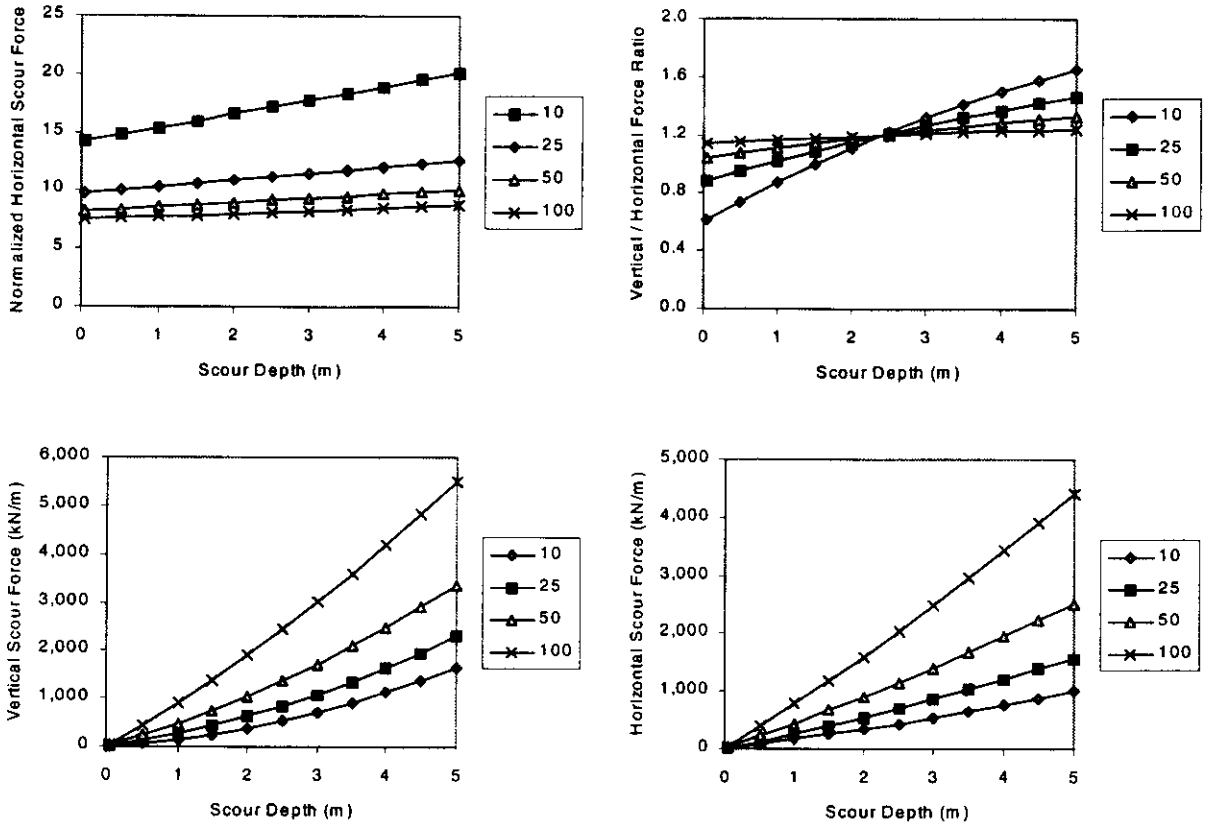

Figure 28. Sensitivity of undrained model to c_u (B=15 m, α=165°, γ'=10 kN/m3)

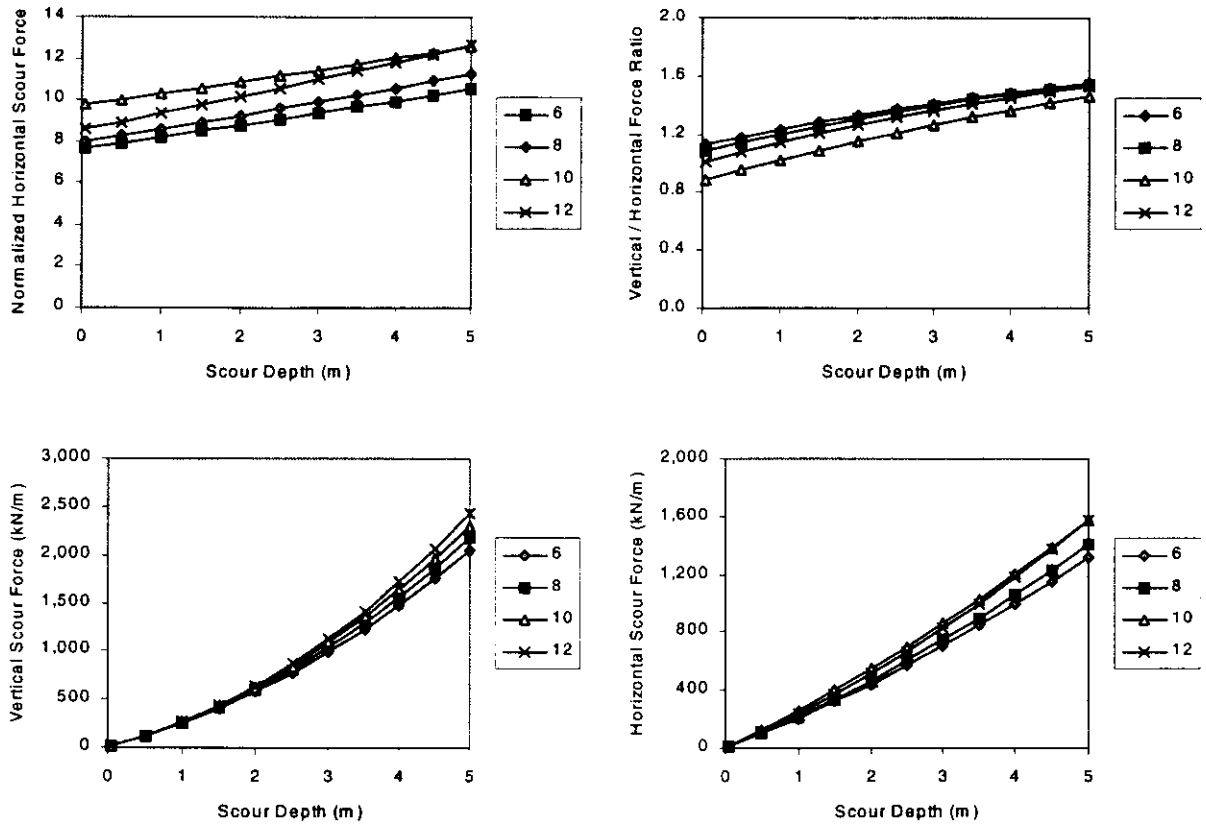

Figure 29. Sensitivity of undrained model to γ' (B=15 m, α=165°, c_u=25 kPa)

REFERENCES

Bea, R. G., Pskar, F. J., Barnes, P. W., and Reimnitz, E. 1985. The role of ice gouging in determining global forces on Arctic structures. Civil Engineeering in the Arctic Offshore, Proceedings of the Conference Arctic '85, ASCE, pp. 251-266.

Been, K., Palmer, A. and Comfort, G. 1990a. Analysis of subscour stresses and probability of ice scour-induced damage for buried submarine pipelines. Volume II. Deterministic model of ice-soil-pipe interaction. PERD and Canada Oil and Gas Lands Administration - Energy, Mines and Resources Indian and Northern Affairs. February.

Been, K., Kosar, K., Hachey, J., Rogers, B.T., and Palmer, A.C. 1990b. Ice scour models. Proceedings of the 9th International Conference on Offshore Mechanics and Arctic Engineering. Volume 5. Pp 179-188.

Beloshapkov, A., Marchenko, A. and Dlugach, A. 1998. Seabed exaration by ice formations. Proceedings of Ice Scour & Arctic Marine Pipelines Workshop, Hokkaido, Japan, 1-5 February. Published by C-CORE, November 1998.

Beloshapkov, A. and Marchenko, A. 1998. Mathematical modeling of ice bottom scouring in Baydaratskaya Bay. 13th International Symposium on Okhotsk Sea and Sea Ice and the Ice Scour and Marine Pipelines Workshop. Abstracts. 1-5 February. Mombetsu, Hokkaido, Japan. Pp 348-353.

C-CORE. 1995a. Pressure Ridge Ice Scour Experiment (PRISE), Phase 3: Centrifuge modeling of ice keel scour, PRISE 01B, Data Report. Contract Report. St. John's, NF. March.

C-CORE. 1995b. Pressure Ridge Ice Scour Experiment (PRISE), Phase 3: Centrifuge modeling of

ice keel scour, PRISE 01C, Data Report. Contract Report. St. John's, NF. April.

C-CORE. 1995c. Pressure Ridge Ice Scour Experiment (PRISE), Phase 3: Centrifuge modeling of ice keel scour, PRISE 03, Data Report. Contract Report. St. John's, NF. January.

C-CORE. 1995d. Pressure Ridge Ice Scour Experiment (PRISE), Phase 3: Centrifuge modeling of ice keel scour, PRISE 04, Data Report. Contract Report. St. John's, NF. January.

C-CORE. 1995e. Pressure Ridge Ice Scour Experiment (PRISE), Phase 3: Centrifuge modeling of ice keel scour, PRISE 05, Data Report. Contract Report. St. John's, NF. January.

C-CORE. 1995f. Pressure Ridge Ice Scour Experiment (PRISE), Phase 3: Centrifuge modeling of ice keel scour, PRISE 06, Data Report. Contract Report. St. John's, NF. March.

C-CORE. 1995g. Pressure Ridge Ice Scour Experiment (PRISE), Phase 3: Centrifuge modeling of ice keel scour, PRISE 08, Data Report. Contract Report. St. John's, NF. April.

C-CORE. 1995h. Pressure Ridge Ice Scour Experiment (PRISE), Phase 3: Centrifuge modeling of ice keel scour, PRISE 09, Data Report. Contract Report. St. John's, NF. March.

C-CORE. 1995i. Pressure Ridge Ice Scour Experiment (PRISE), Phase 3: Centrifuge modeling of ice keel scour, PRISE 10, Data Report. Contract Report. St. John's, NF. March.

Chari, T. R., 1975. Some geotechnical aspects of iceberg grounding. PhD thesis to the Faculty of Engineering and Applied Science, Memorial University of Newfoundland.

Chari, T. R., 1979. Geotechnical aspects of iceberg scours on ocean floors. Canadian Geotechnical Journal, Volume 16, No. 2, pp. 379-390.

Chari, T. R., 1980. A model study of iceberg scouring in the North Atlantic. Journal of Petroleum Technology, December, pp. 2247-2252.

Chari, T. R. and Muthukrisknaiah, K., 1978. Iceberg threat to ocean floor structures. Proceedings, Symposium on Ice Problems, International Association for Hydraulic Research, Lulea, Sweden, pp 421-435.

Chari, T. R., Peters, G. R., and Muthukrishnaiah, K. 1980. Environmental factors affecting iceberg scour estimates. Cold Region Science and Technology, Volume 1, pp. 223-230.

Chari, T. R. and Peters, G. R. 1981. Estimates of iceberg scour depths. In Proceedings of the Symposium on Production and Transportation Systems for the Hibernia Discovery, St. John's, Newfoundland, February, pp. 178-188.

Chari, T. R. and Green, H. P., 1981. Iceberg scour studies in medium dense sands. Proceedings, 6th International Conference on Port and Ocean Engineering under Arctic Conditions, Quebec City, Quebec, Vol. 2, pp. 1012-1019.

Chari, T. R. and Guha, S. N. 1978. A model study of iceberg scouring in North Atlantic. In Proceedings of OTC 78, Volume 3, pp. 2319-2326.

Comfort, G., Abdelnour, R., Trak, B., Menon, B. and Graham, B. 1982. Lake Erie ice scour investigation. Workshop on ice Scouring Sponsored by Snow and Ice Subcommittee, Associate Committee on Geotechnical Research, Technical Memorandum No. 136. 15-19 February. Pp 55-99.

Dunwoody, A. B., Losch, J. A., and Been, K. 1984. Ice/Bern Interactions. 16th Annual Offshore Technology Conference, Houston, Texas.

Fenco. 1975. An analytical study of scour on the sea bottom. Report submitted to Arctic Petroleum Operators Association, April, 1975.

Green, H. P. 1984. Geotechnical modeling of iceberg-seabed interaction. Master of Engineering thesis. Memorial University of Newfoundland, St. John's, NF.

Hettiaratchi, D. R. P., and Reece, A. R. 1975. Boundary wedges in two-dimensional passive soil failure. Geotechnique 25, 2, pp. 297-220.

Lach, P. R. 1996. Centrifuge modeling of large soil deformation due to ice scour. PhD thesis. Memorial University of Newfoundland. St. John's, NF.

Kioka, S. and Saeki, H. 1995. Mechanisms of ice gouging. Proceedings of 5th International Offshore and Polar Engineering Conference (ISOPE), Volume 2, pp. 398-402.

Kioka, S, Terai, Y., Otsuka, N., Honda, H. and Saeki, H. 1998. Mechanical model of ice gouging on sloping sandy beach. The 13th International Symposium on Okhotsk Sea and Sea Ice and the Ice Scour and Arctic Marine Pipelines Workshop, Abstracts. Mombetsu, Hokkaido, Japan. February 1 to 5. Pp 251-256.

Rosenfarb, J. L. and Chen, W. F. 1972. Limit analysis solutions of earth pressure problems. Fritz Eng. Laboratory Report 355..14, Lehigh University, 53 pp.

Sokolovski, V. V. 1965. Statistics of granular media. Pergamon Press, New York, N.Y.

Surkov, G. A. 1995. Method for determining the optimum burial profile for subsea pipeline facilities in freezing seas. Dissertation for a degree of candidate of technical services. Sakhalin Research and Design Institute.

Truskov, P. A., and Surkov, G. A. 1991. Scour depths distribution on the northern Sakhalin offshore. In Proceedings of the 1st International Offshore and Polar Engineering Conference, Edinburgh, UK, pp. 467-470.

Winsor, R., Lach, P. R. and Parsons, G. 1996. Pressure Ridge Ice Scour Experiment, Phase 3c: Extreme Ice Scour Event - Modeling and Interpretation, Milestone 2: Centrifuge Test PRCST01 Data Report. Contract Report 96-C27. St. John's, NF. August.

Winsor, R., and O'Neil, P. 1996a. Pressure Ridge Ice Scour Experiment, Phase 3c: Extreme Ice Scour Event - Modeling and Interpretation, Milestone 2: Centrifuge Test PRSC01 Data Report. Contract Report 96-C32. St. John's, NF. October.

Winsor, R., and O'Neil, P. 1996b. Pressure Ridge Ice Scour Experiment, Phase 3c: Extreme Ice Scour Event - Modeling and Interpretation, Milestone 2: Centrifuge Test PRSC02 Data Report. Contract Report 96-C34. St. John's, NF. November.

Winsor, R., and O'Neil, P. 1996c. Pressure Ridge Ice Scour Experiment, Phase 3c: Extreme Ice Scour Event - Modeling and Interpretation, Milestone 2: Centrifuge Test PRCS02 Data Report. Contract Report 96-C42. St. John's, NF. December.

Winsor, R., and Parsons, G. 1997a. Pressure Ridge Ice Scour Experiment, Phase 3c: Extreme Ice Scour Event - Modeling and Interpretation, Milestone 2: Centrifuge Test PRSA01 Data Report. Contract Report 97-C5. St. John's, NF. April.

Winsor, R., and Parsons, G. 1997b. Pressure Ridge Ice Scour Experiment, Phase 3c: Extreme Ice Scour Event - Modeling and Interpretation, Milestone 2: Centrifuge Test PRSA02 Data Report. Contract Report 97-C6. St. John's, NF. April.

Winsor, R., and Parsons, G. 1997c. Pressure Ridge Ice Scour Experiment, Phase 3c: Extreme Ice Scour Event - Modeling and Interpretation, Milestone 2: Centrifuge Test PRSA03 Data Report. Contract Report 97-C7. St. John's, NF. April.

Winsor, R., and Parsons, G. 1997d. Pressure Ridge Ice Scour Experiment, Phase 3c: Extreme Ice Scour Event - Modeling and Interpretation, Milestone 2: Centrifuge Test PRSA04 Data Report. Contract Report 97-C8. St. John's, NF. April.

Winsor, R., and Parsons, G. 1997e. Pressure Ridge Ice Scour Experiment, Phase 3c: Extreme Ice Scour Event - Modeling and Interpretation, Milestone 2: Centrifuge Test PRSA05 Data Report. Contract Report 97-C14. St. John's, NF. April.